

# Energetic Spectral-Element Time Marching Methods for Phase-Field Nonlinear Gradient Systems

Shiqin Liu<sup>a,b</sup>, Haijun Yu<sup>b,a,\*</sup>

<sup>a</sup>*School of Mathematical Sciences, University of Chinese Academy of Sciences, Beijing 100049, China*

<sup>b</sup>*LSEC & NCMIS, Institute of Computational Mathematics and Scientific/Engineering Computing, Academy of Mathematics and Systems Science, Beijing 100190, China*

---

## Abstract

We propose two efficient energetic spectral-element methods in time for marching nonlinear gradient systems with the phase-field Allen–Cahn equation as an example: one fully implicit nonlinear method and one semi-implicit linear method. Different from other spectral methods in time using spectral Petrov-Galerkin or weighted Galerkin approximations, the presented implicit method employs an energetic variational Galerkin form that can maintain the mass conservation and energy dissipation property of the continuous dynamical system. Another advantage of this method is its superconvergence. A high-order extrapolation is adopted for the nonlinear term to get the semi-implicit method. The semi-implicit method does not have superconvergence, but can be improved by a few Picard-like iterations to recover the superconvergence of the implicit method. Numerical experiments verify that the method using Legendre elements of degree three outperforms the 4th-order implicit-explicit backward differentiation formula and the 4th-order exponential time difference Runge-Kutta method, which were known to have best performances in solving phase-field equations. In addition to the standard Allen–Cahn equation, we also apply the method to a conservative Allen–Cahn equation, in which the conservation of discrete total mass is verified. The applications of the proposed methods are not limited to phase-field Allen–Cahn equations. They are suitable for solving general, large-scale nonlinear dynamical systems.

*Keywords:* spectral-element time marching, energy stable, Allen–Cahn equation, semi-implicit schemes, superconvergence

---

## 1. Introduction

The phase-field method is a highly effective computational tool for modeling and predicting morphological evolutions in material science [1, 2, 3, 4], fluid dynamics [5, 6, 7, 8], biological systems [9, 10, 11, 12], etc. However, the small parameter of interface thickness in phase-field models makes them numerically challenging stiff and nonlinear problems. In this paper, we propose efficient energetic spectral-element time marching methods for phase-field gradient systems, using the following Allen–Cahn equation as an illustrative example:

$$u_t - \varepsilon \Delta u + \frac{1}{\varepsilon} f(u) = 0, \quad x \in \Omega \times [0, T], \quad (1)$$

$$u|_{\partial\Omega} = 0, \quad (2)$$

$$u(x, t) = u_0(x), \quad \text{at } t = 0, \quad (3)$$

---

\*Corresponding author

Email addresses: sqliu@lsec.ac.cc.cn (Shiqin Liu), hyu@lsec.cc.ac.cn (Haijun Yu)

where  $f(u) = F'(u)$  and  $F(u)$  represents a double-well potential, which is typically chosen as

$$F(u) = \frac{1}{4}(1 - u^2)^2. \quad (4)$$

For simplicity, we only analyze the Dirichlet condition (2). It is straightforward to extend the results in this paper to other types of boundary conditions.

Equation (1) is introduced by Allen and Cahn [2] to describe the motion of anti-phase boundary motion in crystalline solids. An important feature of the Allen–Cahn equation is its energy dissipation property: The equation can be viewed as a  $L^2$  gradient flow of the Ginzburg-Landau free energy [1, 13], which is defined as

$$E(u) := \int_{\Omega} \left( \frac{\varepsilon}{2} |\nabla u|^2 + \frac{1}{\varepsilon} F(u) \right) dx. \quad (5)$$

By pairing (1) with  $u_t$  or  $-\varepsilon \Delta u + \frac{1}{\varepsilon} f(u)$ , we find the energy law for (1):

$$\frac{\partial}{\partial t} E(u(t)) = - \int_{\Omega} |u_t|^2 dx = - \int_{\Omega} \left| -\varepsilon \Delta u + \frac{1}{\varepsilon} f(u) \right|^2 dx \leq 0.$$

When solving phase field problems, it is important to verify the algorithms' energy stability property at the discrete level, making energy-stable schemes highly preferable. There are several popular numerical techniques for achieving energy stability for large time step sizes, which can be roughly classified into two categories. The first category maintains original energy (with a possible addition of a diminishing momentum term) dissipation, including methods such as the secant method [14], convex splitting methods [15, 16, 17, 18], and linearly stabilization schemes [19, 20, 21, 22, 23, 24, 25], ETD or IMEX Runge-Kutta methods [26, 27, 28, 29, 30, 31, 32]. The methods in the second category maintain stability of modified energies with auxiliary variables. For example, in invariant energy quadratization (IEQ) [33, 34, 35], the bulk potential is transformed into a quadratic form using a set of new variables, and the nonlinear terms are semi-explicitly treated, resulting in linear and unconditionally stable systems. This approach is a generalization of augmented Lagrange multiplier (ALM) method [36, 37]. The scalar auxiliary variable (SAV) methods [38, 39, 40] are built on a similar methodology, but are more efficient by introducing an auxiliary scalar variable (instead of an auxiliary function in IEQ approach). SAV methods can achieve second-order unconditionally stability and only requires solving linear, decoupled systems with constant coefficients at each time step.

However, designing efficient high order ( $\geq 3$ ) schemes that can keep the mass conservation in machine accuracy and keep energy dissipation with reasonable time step sizes is still a challenging task. In this paper, we introduce an implicit and a semi-implicit spectral-element time marching schemes based on an energetic weak formulation. Let  $H^1 := W^{1,2}(\Omega)$  with  $W^{k,p}(\Omega)$  denoting standard Sobolev space. Here  $\Omega \subset \mathbb{R}^d (d = 2, 3)$  is a bounded domain with  $C^{1,1}$  boundary  $\partial\Omega$  or a convex polygonal domain. We define

$$V_{[s,t]} := H^1(s, t; H_0^1(\Omega)), \quad V_{[s,t]}^{u_0} := \{u \in V_{[s,t]} \mid u(x, s) = u_0(x)\},$$

where  $H_0^1(\Omega) = \{u \in H^1(\Omega), u|_{\partial\Omega} = 0\}$ . The energetic weak form is presented as follows:

$$\text{Find } u \in V_{[0,T]}^{u_0}, \text{ s.t. } \int_0^T (u_t, v_t) + \varepsilon (\nabla u, \nabla v_t) + \frac{1}{\varepsilon} (f(u), v_t) dt = 0, \quad \forall v \in V_{[0,T]}^{u_0}. \quad (6)$$

Here  $(\cdot, \cdot)$  denotes inner product in  $L^2(\Omega)$ . By setting  $v = u$  in (6), we obtain the energy dissipation:

$$E[u(x, T)] - E[u(x, 0)] = - \int_0^T (u_t, u_t) dt \leq 0. \quad (7)$$

We note that taking  $v \in V_{[0,T]}^{u_0}$  in (6) is equivalent to taking  $v_t \in W_{[0,T]} := L^2(0, T; H_0^1(\Omega))$ . We refer the readers to [41, 42] for the regularities of solutions to equation (1). Our schemes are spectral

Galerkin methods based on weak form (6). Comparing to existing spectral time marching method based on Petrov-Galerkin or weighted-Galerkin approach [43, 44], our approach has two obvious advantages: 1) If the continuous equation conserves total mass then the Galerkin methods based on weak form (6) does. 2) Energy dissipation is kept like (7). By utilizing spectral/spectral-element approximation in both time and space, we obtain schemes with an adjustable order and good energy stability.

The remain part of this paper is organized as follows. In Section 2, we present the numerical schemes: one implicit scheme and one semi-implicit scheme, with their major properties and some implementation details. In Section 3, we present standard error estimates for the proposed schemes. Section 4 is devoted to the superconvergence of the implicit scheme and how it can be efficiently solved by using a Picard-like iteration similar to the semi-implicit scheme. Section 5 presents numerical results, where energy stability and superconvergence are numerically verified, and computational efficiency comparison among the proposed methods and some other popular approaches are made. In this section, we also solve the conservative Allen–Cahn equation, which shows our approach can maintain mass conservation to machine accuracy. We end the paper with some concluding remarks in Section 6.

## 2. The energetic spectral-element time marching (ESET) schemes

We now describe space-time Galerkin schemes based on the weak form (6).

We first define finite dimension approximations of  $V_{[s,t]}$  and  $V_{[s,t]}^{u_0}$ :

$$V_{M,N}^{[s,t]} := P_M^0(\Omega) \otimes P_N([s,t]), \quad P_M^0(\Omega) := \{u(x) \in P_M(\Omega), u|_{\partial\Omega} = 0\},$$

$$V_{M,N}^{[s,t],u_0} := \left\{ u \in V_{M,N}^{[s,t]}, u(x,s) = u_0(x) \in P_M^0(\Omega) \right\},$$

where  $P_M(\Omega)$  denotes all polynomials of degree no greater than  $M$  defined on domain  $\Omega$ .

### 2.1. Galerkin approximation on a single element

The Galerkin approximation for (6) is defined as: Find  $h \in V_{M,N}^{[0,T],u_0}$ , s.t.

$$\int_0^T (h_t, v_t) + \varepsilon(\nabla h, \nabla v_t) + \frac{1}{\varepsilon}(f(h), v_t) dt = 0, \quad \forall v \in V_{M,N}^{[0,T],u_0}. \quad (8)$$

Here we use  $h$  to denote numerical solutions. By setting  $v = h$  in (8), we immediately obtain the discrete energy law:

$$E[h(x, T)] - E[h(x, 0)] = - \int_0^T (h_t, h_t) dt \leq 0.$$

The Allen–Cahn equation (1) has an intrinsic time scale  $O(\varepsilon)$ . For problems with long time period  $T \gg \varepsilon$ , a numerical method based on (8) would need to solve a nonlinear system with a very large  $N$ , which is not efficient. Moreover, the solution may not be unique. To obtain efficient methods, we consider instead a spectral-element approach.

### 2.2. Spectral-element Galerkin approximation: the implicit scheme

We first partition the grid for  $t \in [0, T]$ :  $0 = t_0 < t_1 < \dots < t_K = T$ . For simplicity, we consider in this paper only uniform grids:  $t_n = n\tau, n = 0, 1, \dots, K, \tau = T/K$ . Then, on each time interval  $I_n := [t_{n-1}, t_n]$ , we consider a sub-problem that is similar to (8). Denote by  $h^n(x, t)$  the numerical solution on interval  $I_n$ ,  $u(x, t_n)$  the exact solution at  $t_n$ ,  $u^n(x) := h^n(x, t_n)$  the numerical solution at

$t_n$ ,  $V_{M,N}^{n,u^{n-1}} := V_{M,N}^{[t_{n-1},t_n],u^{n-1}}$ . Then, the weak form for the exact solution on interval  $I_n$  reads: Find  $u(x, t) \in V_{[t_{n-1},t_n]}^{u(x,t_{n-1})}$ , s.t.

$$\int_{t_{n-1}}^{t_n} (u_t, v_t) + \varepsilon(\nabla u, \nabla v_t) + \frac{1}{\varepsilon}(f(u), v_t) dt = 0, \quad \forall v \in V_{[t_{n-1},t_n]}^{u(x,t_{n-1})}. \quad (9)$$

The corresponding Galerkin approximation is: Find  $h^n \in V_{M,N}^{n,u^{n-1}}$ , s.t.

$$\int_{t_{n-1}}^{t_n} (h_t^n, v_t) + \varepsilon(\nabla h^n, \nabla v_t) + \frac{1}{\varepsilon}(f(h^n), v_t) dt = 0, \quad \forall v \in V_{M,N}^{n,u^{n-1}}. \quad (10)$$

The above scheme leads to nonlinear algebraic systems to solve, since  $f(\cdot)$  is nonlinear. The advantageous aspect is that if the interval  $[t_{n-1}, t_n]$  is small enough, the system will have a unique solution. Meanwhile, we can choose a smaller  $N$  to represent the solution that satisfies the energy dissipation property. These results are stated in the following theorem.

**Theorem 1.** *Suppose*

$$\max_u |f'(u)| < L. \quad (11)$$

For  $\tau = |t_n - t_{n-1}| \leq \varepsilon/L$ , equation (10) has a unique solution  $h^n$ , and it satisfies the discrete energy law

$$E[h^n(x, t_n)] - E[h^n(x, t_{n-1})] = - \int_{t_{n-1}}^{t_n} (h_t^n, h_t^n) dt \leq 0. \quad (12)$$

The energy stability can be obtained straightforwardly. We leave the proof of uniqueness to Section 4.

**Remark 1.** *The standard double-well potential (4) doesn't satisfy condition (11) in Theorem 1, because  $|f'(u)| \rightarrow \infty$  as  $|u| \rightarrow \infty$ . But, the Allen–Cahn problem (1)–(4) satisfies the maximum principle  $|u(x, t)| \leq 1$  if the initial value  $|u(x, 0)| \leq 1$ , so we can modify the double-well potential (4) to have quadratic growth for  $|u| > 1$  without affecting the exact solution, such that the Lipschitz condition (11) is satisfied. Therefore, it has been a common practice (cf. e.g. [45, 22, 46, 42]) to consider the Allen–Cahn (and Cahn–Hilliard) equation with a truncated quadratic growth double-well potential. For example, following truncation is considered in [47]:*

$$\tilde{F}(u) = \begin{cases} \frac{3M^2 - 1}{2}u^2 - 2M^3u + \frac{1}{4}(3M^4 + 1), & u > M, \\ \frac{1}{4}(u^2 - 1)^2, & u \in [-M, M], \\ \frac{3M^2 - 1}{2}u^2 + 2M^3u + \frac{1}{4}(3M^4 + 1), & u < -M, \end{cases} \quad (13)$$

where  $M \geq 1$  is a parameter. For the Cahn–Hilliard equation, one usually chooses  $M > 1$ . For the Allen–Cahn equation, it is sufficient to choose  $M = 1$ , due to the maximum principle. When  $M = 1$ , (13) reduces to

$$\hat{F}(u) = \begin{cases} (u + 1)^2, & u < -1, \\ (u^2 - 1)^2/4, & -1 \leq u \leq 1, \\ (u - 1)^2, & u > 1. \end{cases} \quad (14)$$

If we use  $\tilde{F}(u)$  to replace  $F(u)$ , then (11) is satisfied with  $L = 3M^2 - 1$ .

To solve the nonlinear system, it is usually necessary to use iterative methods. For example, Newton's method can be applied, which has a fast convergence rate. However, in each sub-iteration of Newton's method, one needs to solve large linear systems with variable coefficients, and the formation and solution of such systems are very expensive.

We propose next a linear scheme with constant coefficients which can be solved efficiently.

### 2.3. Spectral-element Galerkin approximation: the semi-implicit linear scheme

Now, on each sub-interval  $I_n$ , we consider the following semi-implicit Galerkin approximation: Find  $h^n \in V_{M,N}^{n,u^{n-1}}$ , s.t.

$$\int_{t_{n-1}}^{t_n} (h_t^n, v_t) + \varepsilon(\nabla h^n, \nabla v_t) + \frac{S}{\varepsilon}(h^n, v_t) + \frac{1}{\varepsilon}(\hat{f}(\hat{h}^n), v_t) dt = 0, \quad \forall v \in V_{M,N}^{n,u^{n-1}}. \quad (15)$$

Here  $S > 0$  is a stabilization constant to ensure that  $\hat{f}(u) := f(u) - Su$  is concave within the specified region of  $u$  [22]. For the Allen–Cahn equation, the maximum principle implies that  $u(x, t) \in [-1, 1]$  if the initial condition  $u_0(x) \in [-1, 1]$ . By choosing  $S = 2$ ,  $\hat{f}$  is concave for  $u \in [-1, 1]$ . In (15),  $\hat{h}^n$  is defined as the extension of  $h^{n-1}$  from  $I_{n-1}$  to  $I_n$ , for  $n > 1$ . For the first step  $n = 1$ , we can use an implicit scheme or other existing high-order schemes to obtain  $h^1$ . It is easy to verify that (15) forms a linear positive-definite system for the unknown degree of freedom. Note that a single stabilization term can make first order schemes unconditionally energy stable [22], but it is not enough to guarantee unconditional stability for a second-order scheme [23]. Here, we can not prove unconditionally energy stable by adding the stabilization term, but it indeed has some stabilization effect numerically, so we choose to keep (15) in the current form with  $S > 0$  being a tuning parameter.

### 2.4. Implementation

Now we turn to numerical implementation. We use (15) as an example to describe implementation details. We first use a time rescaling

$$t = \frac{1 - \xi}{2} t_{n-1} + \frac{1 + \xi}{2} t_n, \quad \xi \in I := [-1, 1],$$

to transform (15) on interval  $I_n$  to a problem defined on the standard reference interval  $I$ : Find  $h^n \in U_{M,N}^{h_0^n}$ , such that

$$\int_{-1}^1 \frac{2}{\tau} (h_\xi^n, v_\xi) + \varepsilon(\nabla h^n, \nabla v_\xi) + \frac{S}{\varepsilon}(h^n, v_\xi) + \frac{1}{\varepsilon}(\hat{f}(\hat{h}^n), v_\xi) d\xi = 0, \quad \forall v \in U_{M,N}^{h_0^n},$$

$$\hat{h}^n(x, \xi) = h^{n-1}(x, \xi + 2), \quad h^n(x, \xi = -1) = h_0^n(x) := h^{n-1}(x, 1),$$

where  $U_{M,N} := V_{M,N}^{[-1,1]}$ ,  $U_{M,N}^v := V_{M,N}^{[-1,1],v}$ .

We use following compactly-combined Legendre bases for temporal discretization

$$\phi_0(\xi) = 1, \quad \phi_1(\xi) = (1 + \xi)/2, \quad \phi_k(\xi) = L_k(\xi) - L_{k-2}(\xi), \quad k = 2, 3, \dots \quad (16)$$

We note that this kind of compactly combined Legendre bases was introduced by Shen in [48], where  $\{\phi_k, k \geq 2\}$  are used to treat elliptic equations with Dirichlet boundary conditions. Here we include  $\phi_0, \phi_1$  to treat initial value problem. Since  $\phi_k(-1) = \phi_k(1) = 0$  for  $k \geq 2$ , so only  $\phi_0(\xi)$  and  $\phi_1(\xi)$  are used to (efficiently) interpolate the values of a solution at  $\xi = -1, 1$ , which correspond to the initial value of current time interval and next time interval. More details are given in (17)-(18). Similar bases were used for problems with natural and other boundary conditions [23, 49, 34, 50]. We note that, the  $\tau$ -methods proposed by [51] is similar to our method applied to linear equations, but they use different bases leading to dense matrices.

Different types of Galerkin methods can be used for spatial discretization. For simplicity, we focus on one-dimensional and two-dimensional rectangular spatial domains. This allow us to employ similar and highly accuracy spectral methods, ensuring that the spatial discretization error is smaller than temporal discretization error. We use  $\psi_j(x), j = 1, \dots, M$  to denote the spatial bases. Then the numerical solution  $h^n(x, \xi)$  can be represented as:

$$h^n(x, \xi) = \sum_{i=0}^N \sum_{j=1}^M \tilde{h}_{ij}^n \phi_i(\xi) \psi_j(x), \quad \xi \in [-1, 1], \quad x \in \mathbb{R}^d, \quad (17)$$

where  $h^n(x, -1) = \sum_{j=1}^M \tilde{h}_{0j}^n \psi_j(x)$  is known. Denote

$$\begin{aligned} A_x &= (a_{ij}^x), & A_\xi &= (a_{ij}^\xi), & B_x &= (b_{ij}^x), & C_\xi &= (c_{ij}^\xi) \\ a_{ij}^x &= (\psi_i'(x), \psi_j'(x)), & a_{ij}^\xi &= (\phi_i'(\xi), \phi_j'(\xi)), & b_{ij}^x &= (\psi_i(x), \psi_j(x)), & c_{ij}^\xi &= (\phi_i'(\xi), \phi_j(\xi)), \end{aligned}$$

with  $i = 1, \dots, N, j = 1, \dots, M$ . Then in each time interval  $I_n$ , equation (15) leads to a linear algebraic system

$$\frac{2}{\tau} A_\xi H^n B_x + \varepsilon C_\xi H^n A_x + \frac{S}{\varepsilon} C_\xi H^n B_x = \frac{1}{\varepsilon} F + R, \quad (18)$$

where  $H^n = (\tilde{h}_{ij}^n)$ ,  $F = (\tilde{f}_{ij})$ ,  $R = (r_{ij})$ , and

$$\begin{aligned} \tilde{f}_{ij} &= - \int_{-1}^1 (\hat{f}(\hat{h}^n), \psi_j(x)) \phi_i'(\xi) d\xi, \\ r_{ij} &= -\varepsilon \int_{-1}^1 (\nabla h^n(x, -1), \nabla \psi_j(x)) \phi_i'(\xi) d\xi - \frac{S}{\varepsilon} \int_{-1}^1 (h^n(x, -1), \psi_j(x)) \phi_i'(\xi) d\xi. \end{aligned}$$

Note that,  $R$  is related to the initial condition  $h^n(x, -1)$  on interval  $I_n$ , which is known by the continuous condition  $h^n(x, -1) = h^{n-1}(x, 1)$ .

We have two efficient ways to solving the resulting linear system (18). The first one is to use a direct sparse solver, since  $A_\xi$  is diagonal,  $A_x$  and  $B_x$  are sparse, and  $C_\xi$  is a sparse matrix which has  $2N - 1$  non-zero elements in the forming form

$$C_\xi = \begin{pmatrix} a_0 & a_1 & & & \\ -a_1 & 0 & a_2 & & \\ & -a_2 & 0 & \cdots & \\ & & \cdots & \cdots & a_{N-1} \\ & & & a_{N-1} & 0 \end{pmatrix},$$

where  $a_i, i = 0, 1, \dots, N - 1$  are non-zeros. The second way is to use the matrix diagonalization approach [52], which involves solving the generalized eigenvalue problem:

$$A_\xi E = C_\xi E \Lambda,$$

where  $E$  is formed by generalized eigenvectors and  $\Lambda$  is a diagonal matrix composed of generalized eigenvalues. Note that the eigenvalues and eigenvector are complex valued, since  $C_\xi$  is not symmetric. It can be proved that such a diagonalization always exist, see [53] for more details. Setting  $H^n = EV$  in (18), we get

$$\frac{2}{\tau} C_\xi E \Lambda V B_x + \varepsilon C_\xi E V A_x + \frac{S}{\varepsilon} C_\xi E V B_x = \frac{1}{\varepsilon} F + R.$$

Multiplying the above equation by  $E^{-1} C_\xi^{-1}$ , we arrive at

$$\frac{2}{\tau} \Lambda V B_x + \varepsilon V A_x + \frac{S}{\varepsilon} V B_x = E^{-1} C_\xi^{-1} \left( \frac{1}{\varepsilon} F + R \right),$$

which is a series of independent systems that involves only sparse spatial matrices, thus can be solved efficiently using fast spatial solvers. We note that, for large  $N$ , there exist other type of fast solution methods [54].

### 3. Stability and convergence analysis

#### 3.1. Some preliminaries

Denote  $H_0^1(I) = \{u \in H^1(I) : u(\pm 1) = 0\}$ ,  $P_N^0(I) = \{u \in P_N : u(\pm 1) = 0\}$ . We first present some preliminary results.

**Lemma 1.** Suppose that  $h \in H^1([0, \tau])$ , then

$$\int_0^\tau |h(t)|^2 dt \leq 2\tau|h(0)|^2 + 2\tau^2 \int_0^\tau |h_t(t)|^2 dt. \quad (19)$$

$$\int_0^\tau |h(t)|^2 dt \leq 2\tau|h(\tau)|^2 + 2\tau^2 \int_0^\tau |h_t(t)|^2 dt. \quad (20)$$

If  $h(0) = 0$  or  $h(\tau) = 0$ , the estimate can be improved as

$$\int_0^\tau |h(t)|^2 dt \leq \tau^2 \int_0^\tau |h_t(t)|^2 dt. \quad (21)$$

*Proof.* Let  $h(t) = h(0) + g(t)$ , then  $g(0) = 0$ , and

$$\int_0^\tau |h(t)|^2 dt \leq 2\tau|h(0)|^2 + 2 \int_0^\tau |g(t)|^2 dt. \quad (22)$$

For the last term in above equation, we have

$$\int_0^\tau |g(t)|^2 dt = \int_0^\tau \left| \int_0^t g_t(s) ds \right|^2 dt \leq \int_0^\tau \left( \int_0^\tau |g_t(s)| ds \right)^2 dt \leq \int_0^\tau (\sqrt{\tau} \|g_t\|)^2 dt = \tau^2 \|g_t\|^2,$$

where Hölder inequality is used. Substituting the above inequality into (22), we obtain (19). The inequality (20) is obtained by symmetry. (21) is obtained by noticing  $h(t) = g(t)$  with  $g(0) = 0$  or  $g(\tau) = 0$ .  $\square$

**Lemma 2.** Denote by  $L_k(x)$  the Legendre polynomial of degree  $k$ . Then there exist constants  $1 \leq c_k < 2^{2k-1} 3^{2k+1}$ , such that

$$\int_1^3 |L_k(x)|^2 dx = c_k \int_{-1}^1 |L_k(x)|^2 dx, \quad k = 0, 1, \dots \quad (23)$$

In particular

$$c_0 = 1, \quad c_1 = 13, \quad c_2 = 241, \quad c_3 = 5629.$$

*Proof.* Since  $L_k(x), k = 0, 1, \dots$  are orthogonal polynomials defined on the interval  $[-1, 1]$ , so their roots all lie in  $[-1, 1]$ . Furthermore, by  $L_k(1) = 1$ , we know that  $L_k(x) > 0$  for  $x > 1$ . By  $L_0 = 1, L_1(x) = x$ , and the three term recurrence

$$L_{k+1}(x) = \frac{2k+1}{k+1} x L_k(x) - \frac{k}{k+1} L_{k-1}(x), \quad k \geq 1,$$

we have  $L_{k+1}(x) < 2xL_k(x)$ , for  $x \in [1, 3]$ . By  $L_0(x) \equiv 1$  and mathematical induction, we get  $L_k(x) \leq (2x)^k$ , for  $x \in [1, 3]$ . Therefore,

$$\int_1^3 L_k^2(x) dx \leq \int_1^3 2^{2k} x^{2k} dx = \frac{2^{2k}}{2k+1} (3^{2k+1} - 1) < \frac{2^{2k}}{2k+1} 3^{2k+1}, \quad k > 0.$$

Since  $\int_{-1}^1 L_k^2(x) dx = \frac{2}{2k+1}$ , so  $c_k < 2^{2k-1} 3^{2k+1}$ , for  $k > 0$ . The exact values for small  $k$ 's can be obtained by direct calculations. Obvious  $c_0 = 1$ . For  $k = 1, L_1(x) = x$ ,

$$\int_1^3 x^2 dx = \frac{1}{3} x^3 \Big|_1^3 = \frac{26}{3}, \quad \text{which leads to } c_1 = \frac{26}{3} / \frac{2}{3} = 13.$$

For  $k = 2$ ,  $L_2(x) = \frac{1}{2}(3x^2 - 1)$

$$\int_1^3 \frac{1}{4}(9x^4 - 6x^2 + 1)dx = \left(\frac{9}{20}x^5 - \frac{1}{2}x^3 + \frac{x}{4}\right)\Big|_1^3 = \frac{482}{5}, \quad \text{which leads to } c_2 = \frac{482}{5}/\frac{2}{5} = 241.$$

For  $k = 3$ ,  $L_3(x) = \frac{1}{2}(5x^3 - 3x)$

$$\int_1^3 \frac{1}{4}(5x^3 - 3x)^2 dx = \frac{11258}{7}, \quad \text{which leads to } c_3 = \frac{11258}{7}/\frac{2}{7} = 5629.$$

□

**Lemma 3.** Suppose that  $h \in P_N([0, 2\tau])$ , then

$$\int_\tau^{2\tau} |h(t)| dt \leq C_N \sqrt{\tau} \left( \int_0^\tau |h(t)|^2 dt \right)^{1/2}, \quad (24)$$

where  $C_N = \sqrt{\sum_{k=0}^N c_k}$ . In particular  $C_0 = 1$ ,  $C_1 = \sqrt{14} \cong 3.7$ ,  $C_2 = \sqrt{255} \sim 16.0$ ,  $C_3 = \sqrt{5884} \sim 76.7$ .

*Proof.* First define

$$\varphi_k(t) = \sqrt{\frac{2k+1}{\tau}} L_k\left(\frac{2t}{\tau} - 1\right),$$

where  $L_k(x)$  is Legendre polynomial of degree  $k$ . It is easy to verify that  $\{\varphi_k(t)\}$  compose of a set of orthonormal bases in  $L^2([0, \tau])$ :

$$\int_0^\tau \varphi_k(t) \varphi_j(t) dt = \int_{-1}^1 \frac{\sqrt{(2k+1)(2j+1)}}{\tau} L_k(\xi) L_j(\xi) \frac{\tau}{2} d\xi = \delta_{jk}.$$

Then, by using Lemma 2, we have

$$\int_\tau^{2\tau} |\varphi_k(t)|^2 dt = \frac{2k+1}{2} \int_1^3 |L_k(\xi)|^2 d\xi = c_k \frac{2k+1}{2} \int_{-1}^1 |L_k(\xi)|^2 d\xi = c_k. \quad (25)$$

By expanding  $h(t)$  as  $h(t) = \sum_{k=0}^N b_k \varphi_k(t)$ , we get

$$\int_0^\tau |h(t)|^2 dt = \sum_{k=0}^N b_k^2,$$

and

$$\begin{aligned} \int_\tau^{2\tau} |h(t)| dt &\leq \sum_{k=0}^N |b_k| \int_\tau^{2\tau} |\varphi_k| dt \leq \sum_{k=0}^N |b_k| \sqrt{\tau} \left( \int_\tau^{2\tau} |\varphi_k|^2 dt \right)^{1/2} \\ &= \sum_{k=0}^N |b_k| \sqrt{\tau} \sqrt{c_k} \leq \sqrt{\tau \sum_{k=0}^N c_k} \left( \int_0^\tau |h(t)|^2 dt \right)^{1/2} \\ &= C_N \sqrt{\tau} \left( \int_0^\tau |h(t)|^2 dt \right)^{1/2}. \end{aligned}$$

The proof is complete. □



Next we present several lemmas regarding projection error. Let  $w^{\alpha,\beta}(t) := (1-t)^\alpha(1+t)^\beta$  with  $\alpha, \beta > -1$ . Introduce the non-uniformly Jacobi-weighted Sobolev space:

$$B_{\alpha,\beta}^m(I) = \{ u : \partial_t^k u \in L_{w^{\alpha+k,\beta+k}}^2(I), 0 \leq k \leq m \}, m \in \mathbb{N}, \quad (26)$$

equipped with the inner product, norm and semi-norm

$$(u, v)_{B_{\alpha,\beta}^m} = \sum_{k=0}^m (\partial_t^k u, \partial_t^k v)_{w^{\alpha+k,\beta+k}},$$

$$\|u\|_{B_{\alpha,\beta}^m} = (u, u)_{B_{\alpha,\beta}^m}^{1/2}, \quad |u|_{B_{\alpha,\beta}^m} = \|\partial_t^m u\|_{w^{\alpha+m,\beta+m}}.$$

For given temporal or spatial domain  $\Omega$ , we define

$$a(u, v) = \int_{\Omega} \nabla u(\xi) \cdot \nabla v(\xi) d\xi.$$

Consider the orthogonal projection  $\Pi_N^0 : H_0^1(\Omega) \mapsto P_N^0(\Omega)$ , defined by

$$a(\Pi_N^0 u - u, v) = 0, \quad \forall v \in P_N^0(\Omega). \quad (27)$$

For the one-dimensional case, we have the following lemma.

**Lemma 4.** [55, 56] *If  $u \in H_0^1(I)$  and  $\partial_\xi u \in B_{0,0}^{m-1}(I)$ , then for  $1 \leq m \leq N+1$  and  $\mu = 0, 1$ ,*

$$\|\Pi_N^0 u - u\|_\mu \leq c \sqrt{\frac{(N-m+1)!}{N!}} (N+m)^{\mu-(m+1)/2} \|\partial_\xi^m u\|_{w^{m-1,m-1}}, \quad (28)$$

where  $c$  is a positive constant independent of  $m, N$  and  $u$ .

Define linear interpolation operator  $\mathcal{I}_1^n : C^0(I_n) \mapsto P_1(I_n)$  as

$$\mathcal{I}_1^n u(t) = \frac{t_n - t}{\tau} u(t_{n-1}) + \frac{t - t_{n-1}}{\tau} u(t_n). \quad (29)$$

Define projection  $\Pi_N^{0,n} : H_0^1(I_n) \mapsto P_N^0(I_n)$  as

$$\int_{I_n} (u - \Pi_N^{0,n} u)'(t) v'(t) dt = 0, \quad \forall v \in P_N^0(I_n). \quad (30)$$

Then, define operator  $\Pi_N^n : H^1(I_n) \mapsto P_N(I_n)$  as

$$\Pi_N^n u(t) = \mathcal{I}_1^n u(t) + \Pi_N^{0,n}(u - \mathcal{I}_1^n u). \quad (31)$$

By using Lemma 4, the following result can be obtained.

**Lemma 5.** *If  $u \in H^1(I_n)$  and  $\partial_t u \in B_{0,0}^{m-1}(I_n)$ , then for  $\mu = 0, 1$ , we have*

$$\|\partial_t^\mu (\Pi_N^n u - u)\|_{L^2(I_n)} \leq c \left(\frac{\tau}{2}\right)^{m-\mu} \sqrt{\frac{(N-m+1)!}{N!}} (N+m)^{\mu-(m+1)/2} \|\partial_t^m u\|_{L_{w^{m-1,m-1}}^2(I_n)}, \quad (32)$$

for  $1 \leq m \leq N+1$ , where  $c$  is a positive constant independent of  $m, N$  and  $u$ . In particular, when  $m = N+1$ , we have

$$\|\partial_t^\mu (\Pi_N^n u - u)\|_{L^2(I_n)} \leq c \left(\frac{\tau}{2}\right)^{N+1-\mu} (2\pi N)^{-1/4} \left(\frac{\sqrt{e/2}}{N}\right)^N \left(\frac{1}{2N+1}\right)^{1-\mu} \|\partial_t^{N+1} u\|_{L_{w_{N,N}}^2(I_n)}. \quad (33)$$

In space, we consider similar projection  $\Pi_M^0 : H_0^1(\Omega) \rightarrow P_M^0(\Omega)$ . We assume the solution is smooth and a large enough  $M$  is used, such that the spatial projection error is small comparing to temporal discretization error:

$$\|\nabla^\mu (\Pi_M^0 u - u)\| \leq cM^{-r} \leq c\tau^{2N}, \quad \mu = 0, 1. \quad (34)$$

### 3.2. Energy stability of the semi-implicit linear ESET method

We first introduce following shorthand notations:

$$(u, v)_n := \int_{t_{n-1}}^{t_n} \int_{\Omega} uv \, dxdt, \quad \|u\|_n^2 := \int_{t_{n-1}}^{t_n} \int_{\Omega} u^2 \, dxdt. \quad (35)$$

We use  $u(t)$  in places of  $u(x, t)$  for notation simplicity. Our first result regarding the energy stability of scheme (15) is given in following theorem.

**Theorem 2.** *Under the condition*

$$\tau \frac{L}{\varepsilon} \leq \frac{\sqrt{14}}{4\sqrt{2 + C_{N-1}^2}}, \quad (36)$$

*the following energy dissipation law*

$$\hat{E}^{n+1} \leq \hat{E}^n, \quad \forall n \geq 1, \quad (37)$$

*holds for scheme (15), where*

$$\hat{E}^n = E(h^n(t_n)) + \frac{\tau^2 L^2 C_{N-1}^2}{2\varepsilon^2} \|h_t^n\|_n^2. \quad (38)$$

*Proof.* We only consider the case  $S = 0$ . The analysis to case  $S \neq 0$  is similar. By taking  $v_t = h_t^n$  in (15), we obtain

$$\|h_t^n\|_n^2 + \left(\frac{d}{dt} E(h^n), 1\right)_n = \frac{1}{\varepsilon} (f(h^n) - f(\hat{h}^n), h_t^n)_n \leq \frac{L}{\varepsilon} (|h^n - \hat{h}^n|, |h_t^n|)_n. \quad (39)$$

Here the that  $f(u) = \hat{f}(u)$  when  $S = 0$  is used. Since  $h^n(t_{n-1}) = \hat{h}^n(t_{n-1})$ , we have

$$|(h^n - \hat{h}^n)(t)| \leq \int_{t_{n-1}}^t |h_t^n(s) - \hat{h}_t^n(s)| ds \leq \int_{t_{n-1}}^t |h_t^n(s)| + |\hat{h}_t^n(s)| ds, \quad t \in [t_{n-1}, t_n].$$

Plugging the above result into (39), then for the first term on the right hand side, we have

$$\left(\int_{t_{n-1}}^t |h_t^n| ds, |h_t^n|\right)_n = \frac{1}{2} \left(\int_{t_{n-1}}^{t_n} |h_t^n| ds, |h_t^n|\right)_n \leq \frac{1}{2} (\sqrt{\tau} \|h_t^n\|_n, |h_t^n|)_n \leq \tau^2 \|h_t^n\|_n^2 + \frac{1}{16} \|h_t^n\|_n^2,$$

where Hölder and Cauchy inequalities are used. For the second term, we do similar estimate and using Lemma 3 to get

$$\left(\int_{t_{n-1}}^t |\hat{h}_t^n| ds, |h_t^n|\right)_n \leq (C_{N-1} \sqrt{\tau} \|h_t^{n-1}\|_{n-1}, |h_t^n|)_n \leq \frac{\tau^2 C_{N-1}^2}{2} \|h_t^{n-1}\|_{n-1}^2 + \frac{1}{2} \|h_t^n\|_n^2, \quad (40)$$

Putting these results into (39), we obtain the discrete energy dissipation relation

$$E(h^n(t_n)) + \frac{\tau^2 C_{N-1}^2 L^2}{2\varepsilon^2} \|h_t^n\|_n^2 \leq E(h^n(t_{n-1})) + \frac{\tau^2 C_{N-1}^2 L^2}{2\varepsilon^2} \|h_t^{n-1}\|_{n-1}^2 - \left(\frac{7}{16} - \frac{\tau^2 L^2 C_{N-1}^2}{\varepsilon^2} \frac{C_{N-1}^2 + 2}{2}\right) \|h_t^n\|_n^2.$$

We obtain desired energy dissipation under condition (36).  $\square$

### 3.3. Convergence analysis

#### 3.3.1. A standard error estimate for the implicit ESET scheme

Let  $h^n, u(t)$  be the solution of equation (10) and (9), correspondingly. Denote by

$$e^n(t) = h^n(t) - u(t) = \rho^n + \pi^n, \quad \rho^n(t) = h^n(t) - \Pi^n u(t), \quad \pi^n(t) = \Pi^n u(t) - u(t),$$

where  $\Pi^n u := \Pi_N^n \Pi_M^0 u$  is a spatial-temporal projection operator. By Lemma 5 and assumption (34), we have

$$\|\nabla^\mu \pi^n\| \leq \|\nabla^\mu (u - \Pi_M^0 u)\| + \|\nabla^\mu (\Pi_M^0 u - \Pi_N^n \Pi_M^0 u)\| \leq cM^{-r} + c\tau^{N+1}, \quad \mu = 0, 1, \quad (41)$$

where  $c$  is a general constant. Since  $\|\nabla^\mu e^n\| = \|\nabla^\mu \rho^n\| + \|\nabla^\mu \pi^n\|$ , to get a  $H_0^1(\Omega)$  upper bound of the numerical error, we only need to estimate  $\|\nabla^\mu \rho^n\|$ , for which we have the following result.

**Theorem 3.** *Following error estimates hold for the implicit ESET scheme (10):*

$$\|\rho^n(t_n)\|^2 + \frac{\varepsilon^2}{2L} \|\nabla \rho^n(t_n)\|^2 + \sum_{k=1}^n D_\tau \|\rho_t^k\|_k^2 \leq \sum_{k=1}^n e^{D_2 k \tau} E_p^k(\tau), \quad \forall \tau \leq \frac{\varepsilon}{4\sqrt{2}L}. \quad (42)$$

where  $D_\tau = \frac{\varepsilon}{4L} - \frac{8\tau^2 L}{\varepsilon}$ ,  $D_2 = \frac{8L}{\varepsilon}$ , and

$$E_p^n(\tau) = 6\|\partial_t(\Pi_M^0 - I_{id})\Pi_N^n u\|_n^2 + 6\varepsilon^2 \|\nabla^2(\Pi_N^n - I_{id})\Pi_M^0 u\|_n^2 + \frac{6L^2}{\varepsilon^2} \|\pi^n\|_n^2, \quad (43)$$

where  $I_{id}$  stands for identity operator. By Lemma 5 and assumption on spatial projection error (34), we have  $E_p^n(\tau) < \mathcal{O}(\tau M^{-2r} + \tau^{2N+3})$ . So the  $H_0^1(\Omega)$  numerical error at a time  $t$  is of order  $\mathcal{O}(M^{-r} + \tau^{N+1})$ .

*Proof.* By taking the difference of (9) and (10), we get

$$(h_t^n - u_t, v_t)_n + \varepsilon(\nabla(h^n - u), \nabla v_t)_n + \frac{1}{\varepsilon}(f(h^n) - f(u), v_t)_n = 0,$$

which leads to

$$(\rho_t^n + \pi_t^n, v_t)_n + \varepsilon(\nabla(\rho^n + \pi^n), \nabla v_t)_n + \frac{1}{\varepsilon}(f'(\zeta^n)(\rho^n + \pi^n), v_t)_n = 0,$$

where  $\zeta^n = \zeta^n(x, t)$  is some value between  $u(x, t)$  and  $h^n(x, t)$ . By taking  $v = \rho^n$ , we get

$$(\rho_t^n + \pi_t^n, \rho_t^n)_n + \varepsilon(\nabla(\rho^n + \pi^n), \nabla \rho_t^n)_n + \frac{1}{\varepsilon}(f'(\zeta^n)(\rho^n + \pi^n), \rho_t^n)_n = 0. \quad (44)$$

Rearranging the above equation yields

$$(\rho_t^n, \rho_t^n)_n + \frac{\varepsilon}{2} \|\nabla \rho^n(t_n)\|^2 - \frac{\varepsilon}{2} \|\nabla \rho^n(t_{n-1})\|^2 = R_1 + R_2 + R_3, \quad (45)$$

where Using the definition of projection and Cauchy-Schwartz inequality, we obtain

$$|R_1| = |(\partial_t(\Pi_M^0 - I_{id})\Pi_N^n u, \rho_t^n)_n| \leq \frac{1}{2\eta_1} \|\partial_t \pi_M^n\|_n^2 + \frac{\eta_1}{2} \|\rho_t^n\|_n^2, \quad 0 < \eta_1, \quad (46)$$

$$|R_2| = |-\varepsilon(\nabla((\Pi_N^n - I_{id})\Pi_M^0 u), \nabla \rho_t^n)_n| \leq \frac{\varepsilon^2}{2\eta_2} \|\nabla^2 \pi_N^n\|_n^2 + \frac{\eta_2}{2} \|\rho_t^n\|_n^2, \quad 0 < \eta_2, \quad (47)$$

$$|R_3| \leq \frac{L^2}{\varepsilon^2} \frac{1}{2\eta_3} \|\rho^n\|_n^2 + \frac{\eta_3}{2} \|\rho_t^n\|_n^2 + \frac{L^2}{\varepsilon^2} \frac{1}{2\eta_4} \|\pi^n\|_n^2 + \frac{\eta_4}{2} \|\rho_t^n\|_n^2, \quad 0 < \eta_3, \eta_4, \quad (48)$$

where  $\pi_M^n = (\Pi_M^0 - I_{id})\Pi_N^n u$ ,  $\pi_N^n = (\Pi_N^n - I_{id})\Pi_M^0 u$ . To control the  $\|\rho^n\|_n^2$  term, we use Lemma 1 to get

$$\|\rho^n\|_n^2 \leq 2\tau\|\rho^n(t_{n-1})\|_n^2 + 2\tau^2\|\rho_t^n\|_n^2. \quad (49)$$

Combining the estimates (45)-(49), we have

$$\begin{aligned} & (\rho_t^n, \rho_t^n)_n + \frac{\varepsilon}{2}\|\nabla\rho^n(t_n)\|^2 - \frac{\varepsilon}{2}\|\nabla\rho^n(t_{n-1})\|^2 \\ & \leq \frac{\eta_1 + \eta_2 + \eta_3 + \eta_4}{2}\|\rho_t^n\|_n^2 + \frac{1}{2\eta_1}\|\pi_t^n\|_n^2 + \frac{\varepsilon^2}{2\eta_2}\|\nabla^2\pi_N^n\|_n^2 + \frac{L^2}{\varepsilon^2}\frac{1}{2\eta_4}\|\pi^n\|_n^2 + \frac{L^2}{\varepsilon^2}\frac{1}{2\eta_3}\|\rho^n\|_n^2 \\ & \leq \left(\frac{\eta_1 + \eta_2 + \eta_3 + \eta_4}{2} + \frac{L^2\tau^2}{\eta_3\varepsilon^2}\right)\|\rho_t^n\|_n^2 + \frac{L^2\tau}{\eta_3\varepsilon^2}\|\rho^n(t_{n-1})\|^2 \\ & \quad + \frac{1}{2\eta_1}\|\pi_t^n\|_n^2 + \frac{\varepsilon^2}{2\eta_2}\|\nabla^2\pi_N^n\|_n^2 + \frac{L^2}{2\eta_4\varepsilon^2}\|\pi^n\|_n^2. \end{aligned}$$

Setting  $\eta_3 = 1/4$ ,  $\eta_1 = \eta_2 = \eta_4 = 1/12$ , we obtain

$$\begin{aligned} & \left(\frac{3}{4} - \frac{4\tau^2L^2}{\varepsilon^2}\right)\|\rho_t^n\|_n^2 + \frac{\varepsilon}{2}\|\nabla\rho^n(t_n)\|^2 - \frac{\varepsilon}{2}\|\nabla\rho^n(t_{n-1})\|^2 \leq \frac{4\tau L^2}{\varepsilon^2}\|\rho^n(t_{n-1})\|^2 \\ & \quad + 6\|\pi_t^n\|_n^2 + 6\varepsilon^2\|\nabla^2\pi_N^n\|_n^2 + \frac{6L^2}{\varepsilon^2}\|\pi^n\|_n^2. \end{aligned} \quad (50)$$

Notice that

$$\begin{aligned} \|\rho^n(t_n)\|^2 - \|\rho^n(t_{n-1})\|^2 & = \int_{t_{n-1}}^{t_n} 2(\rho^n, \rho_t^n)dt \leq \frac{\varepsilon}{2L}\|\rho_t^n\|_n^2 + \frac{2L}{\varepsilon}\|\rho^n\|_n^2 \\ & \leq \frac{4L\tau}{\varepsilon}\|\rho^n(t_{n-1})\|^2 + \frac{\varepsilon}{L}\left(\frac{1}{2} + \frac{4\tau^2L^2}{\varepsilon^2}\right)\|\rho_t^n\|_n^2. \end{aligned} \quad (51)$$

Summing up estimate (51) with (50) multiplied by  $\frac{\varepsilon}{L}$ , we get

$$\|\rho^n(t_n)\|^2 - \|\rho^n(t_{n-1})\|^2 + D\tau\|\rho_t^n\|_n^2 + \frac{\varepsilon^2}{2L}\|\nabla\rho^n(t_n)\|^2 - \frac{\varepsilon^2}{2L}\|\nabla\rho^n(t_{n-1})\|^2 \leq D_2\tau\|\rho^n(t_{n-1})\|^2 + E_p^n(\tau).$$

By a discrete Grönwall's inequality and the fact  $\rho^1(t_0) = 0$ , we obtain the desired estimate (42).  $\square$

### 3.3.2. Error estimate for the semi-implicit linear ESET scheme

Let  $h^n$ ,  $u(t)$  be the solution of equation (15) and (9), correspondingly. We again do following error splitting

$$e^n(t) = h^n(t) - u(t) = \rho^n + \pi^n, \quad \rho^n(t) = h^n(t) - \Pi^n u(t), \quad \pi^n(t) = \Pi^n u(t) - u(t).$$

The a priori projection error  $\pi^n$  is the same as in the implicit scheme, so we only need to estimate the  $\rho^n$  term.

The challenging part for the semi-implicit ESET scheme is the extrapolation term  $\hat{h}^n$ . To make it easier, we introduce a mixed-type projection: we still use the spatial project  $\Pi_M^0$  as in the fully implicit ESET scheme, but for temporal "projection", we use finite-term Taylor series. More precisely, we define  $\hat{\Pi}^n = \mathcal{T}_N^n \Pi_M^0$ , where  $\mathcal{T}_N^n : C^{N+1} \mapsto P_N$  is defined as

$$(\mathcal{T}_N^n u)(t) := \sum_{k=0}^N \frac{1}{k!} u^{(k)}(t_{n-1})(t - t_{n-1})^k, \quad \forall t \in I_n \cup I_{n-1}. \quad (52)$$

It is easy to show that

$$\|u - \mathcal{T}_N^n u\|_\alpha \leq \frac{\tau^{N+1}}{(N+1)!} \|u^{(N+1)}\|_\alpha, \quad \alpha = n, n-1. \quad (53)$$

By using  $\hat{\Pi}^n$  and a similar procedure for implicit scheme, we can get the following result.

**Theorem 4.** *The following error estimates hold for the semi-implicit linear ESET scheme (15):*

$$\begin{aligned} \|\rho^n(t_n)\|^2 + \frac{\varepsilon^2}{2L} \|\nabla \rho^n(t_n)\|^2 + \sum_{k=1}^n D_\tau \|\rho_t^k\|_k^2 + D_3 \tau \|\rho_t^n\|_n^2 &\leq \sum_{k=1}^n e^{D_2 k \tau} \hat{E}_p^k(\tau) \\ &+ \|\rho^1(t_1)\|^2 + \frac{\varepsilon^2}{2L} \|\nabla \rho^1(t_1)\|^2 + D_3 \tau \|\rho_t^1\|_1^2, \quad \forall \tau \leq \frac{\varepsilon}{4L\sqrt{6C_{N-1}^2 + 1}}, \quad n \geq 2, \end{aligned} \quad (54)$$

where  $D_\tau = \frac{\varepsilon}{L}(\frac{1}{4} - \frac{4\tau^2 L^2(1+6C_{N-1}^2)}{\varepsilon^2})$ ,  $D_2 = \frac{8L}{\varepsilon}$ ,  $D_3 = \frac{24L\tau C_{N-1}^2}{\varepsilon}$ , and

$$\begin{aligned} \hat{E}_p^k &= 6\|\partial_t \pi_M^n\|_n^2 + 6\varepsilon^2 \|\nabla^2 \pi_N^n\|_n^2 + \frac{4L^2 \tau^2}{\varepsilon^2} \|\pi^n(t_{n-1})\|^2 \\ &+ \frac{12L^2 \tau^2 C_{N-1}^2}{\varepsilon^2} (\|\hat{\pi}_t^n\|_{n-1}^2 + 2\|\partial_t(\hat{\Pi}^n u - \Pi^{n-1} u)\|_{n-1}^2). \end{aligned} \quad (55)$$

*Proof.* By taking the difference of (9) and (15), and taking  $v = \rho_t^n$ , we obtain

$$(\rho_t^n + \pi_t^n, \rho_t^n)_n + \varepsilon(\nabla \rho^n, \nabla \rho_t^n)_n + \varepsilon(\nabla \pi^n, \nabla \rho_t^n)_n = -\frac{1}{\varepsilon}(f(u) - f(\hat{h}^n), \rho_t^n)_n.$$

Rearranging the above equation to obtain

$$\|\rho_t^n\|_n^2 + \frac{\varepsilon}{2} \|\nabla \rho^n(t_n)\|^2 - \frac{\varepsilon}{2} \|\nabla \rho^n(t_{n-1})\|^2 = R_1 + R_2 + R_3, \quad (56)$$

where  $R_1 = -(\pi_t^n, \rho_t^n)_n$ ,  $R_2 = -\varepsilon(\nabla \pi^n, \nabla \rho_t^n)_n$ . There are same as in the implicit ESET scheme, can be handled similarly. The  $R_3$  term is

$$R_3 = -\frac{1}{\varepsilon}(f'(\zeta^n)(\hat{h}^n - u), \rho_t^n)_n.$$

For  $\hat{h}^n - u$  we use following splitting

$$\hat{h}^n - u = \hat{\rho}^n + \hat{\pi}^n, \quad \hat{\rho}^n(t) = \hat{h}^n(t) - \hat{\Pi}^n u(t), \quad \hat{\pi}^n(t) = \hat{\Pi}^n u(t) - u(t).$$

Then we have

$$\begin{aligned} |R_3| &\leq \frac{L}{\varepsilon} (|\hat{\rho}^n + \hat{\pi}^n|, |\rho_t^n|)_n \\ &\leq \frac{L}{\varepsilon} (|\hat{\rho}^n(t_{n-1}) + \hat{\pi}^n(t_{n-1})| + \int_{t_{n-1}}^t |\hat{\rho}_t^n(s) + \hat{\pi}_t^n(s)| ds, |\rho_t^n|)_n \\ &\leq \frac{L^2 \tau}{\varepsilon^2 \eta_5} (\|\rho^n(t_{n-1})\|^2 + \|\pi^n(t_{n-1})\|^2) + \frac{L^2 \tau^2 C_{N-1}^2}{\varepsilon^2 \eta_6} (\|\hat{\rho}_t^n\|_{n-1}^2 + \|\hat{\pi}_t^n\|_{n-1}^2) + \frac{\eta_5 + \eta_6}{2} \|\rho_t^n\|_n^2, \end{aligned} \quad (57)$$

where the fact  $\rho^n(t_{n-1}) = \hat{\rho}^n(t_{n-1})$ ,  $\pi^n(t_{n-1}) = \hat{\pi}^n(t_{n-1})$ , and Lemma 3 are used. The term  $\|\hat{\rho}_t^n\|_{n-1}^2$  can be further estimated by

$$\begin{aligned} \|\hat{\rho}_t^n\|_{n-1}^2 &= \|\partial_t(h^{n-1} - \hat{\Pi}^n u)\|_{n-1}^2 \leq 2\|\partial_t(h^{n-1} - \Pi^{n-1} u)\|_{n-1}^2 + 2\|\partial_t(\hat{\Pi}^n u - \Pi^{n-1} u)\|_{n-1}^2 \\ &= 2\|\rho_t^{n-1}\|_{n-1}^2 + 2\|\partial_t(\hat{\Pi}^n u - \Pi^{n-1} u)\|_{n-1}^2 \end{aligned} \quad (58)$$

Combining the estimates (46), (47), (56), (57) and (58), then taking  $\eta_5 = 1/4$ ,  $\eta_1 = \eta_2 = \eta_6 = 1/12$ , we obtain

$$\begin{aligned} \frac{3}{4} \|\rho_t^n\|_n^2 + \frac{\varepsilon}{2} \|\nabla \rho^n(t_n)\|^2 - \frac{\varepsilon}{2} \|\nabla \rho^n(t_{n-1})\|^2 \\ \leq \frac{4L^2 \tau}{\varepsilon^2} \|\rho^n(t_{n-1})\|^2 + \frac{24L^2 \tau^2 C_{N-1}^2}{\varepsilon^2} \|\rho_t^{n-1}\|_{n-1}^2 + 6\|\partial_t \pi_M^n\|_n^2 + 6\varepsilon^2 \|\nabla^2 \pi_N^n\|_n^2 \\ + \frac{4L^2 \tau}{\varepsilon^2} \|\pi^n(t_{n-1})\|^2 + \frac{12L^2 \tau^2 C_{N-1}^2}{\varepsilon^2} (\|\hat{\pi}_t^n\|_{n-1}^2 + 2\|\partial_t(\hat{\Pi}^n u - \Pi^{n-1} u)\|_{n-1}^2). \end{aligned} \quad (59)$$

Multiplying the above equation by  $\frac{\varepsilon}{L}$ , then summing the results with (51), we reach to

$$\begin{aligned} & \|\rho^n(t_n)\|^2 - \|\rho^n(t_{n-1})\|^2 + D_\tau \|\rho_t^n\|_n^2 + D_3 \tau \|\rho_t^n\|_n^2 + \frac{\varepsilon^2}{2L} \|\nabla \rho^n(t_n)\|^2 - \frac{\varepsilon^2}{2L} \|\nabla \rho^n(t_{n-1})\|^2 \\ & \leq D_2 \tau \|\rho^n(t_{n-1})\|^2 + D_3 \tau \|\rho_t^{n-1}\|_{n-1}^2 + \hat{E}_p^n(\tau). \end{aligned} \quad (60)$$

By a discrete Grönwall's inequality we obtain the desired estimate (54).  $\square$

#### 4. The semi-implicit iterative solver for the implicit scheme and superconvergence

Now we consider the semi-implicit ESET scheme as an iterative solver for the implicit ESET scheme: Find  $h^{n,k} \in V_{M,N}^{n,u^{n-1}}$ , s.t.

$$\int_{t_{n-1}}^{t_n} (h_t^{n,k}, \phi_t) + \varepsilon (\nabla h^{n,k}, \nabla \phi_t) + \frac{1}{\varepsilon} (f(h^{n,k-1}), \phi_t) dt = 0, \quad \forall \phi \in V_{M,N}^{n,0}, \quad (61)$$

for  $k = 1, \dots, N$ , where  $h^{n,0}(t) = \hat{h}^n(t) := h^{n-1}(t)$ .

##### 4.1. Convergence of the iteration

By taking difference of (61) with  $k$  and  $k-1$ , and denoting  $d^{n,k} = h^{n,k} - h^{n,k-1}$ , we have

$$\int_{t_{n-1}}^{t_n} (d_t^{n,k}, \phi_t) + \varepsilon (\nabla d^{n,k}, \nabla \phi_t) + \frac{1}{\varepsilon} (f(h^{n,k-1}) - f(h^{n,k-2}), \phi_t) dt = 0, \quad \forall \phi \in V_{M,N}^{n,0},$$

which leads to

$$\int_{t_{n-1}}^{t_n} (d_t^{n,k}, \phi_t) + \varepsilon (\nabla d^{n,k}, \nabla \phi_t) + \frac{1}{\varepsilon} (f'(\zeta^n) d^{n,k-1}, \phi_t) dt = 0, \quad \forall \phi \in V_{M,N}^{n,0}.$$

By taking  $\phi_t = d_t^{n,k}$ , we obtain

$$\|d_t^{n,k}\|_n^2 + \frac{\varepsilon}{2} \|\nabla d^{n,k}(t_n)\|^2 - \frac{\varepsilon}{2} \|\nabla d^{n,k}(t_{n-1})\|^2 \leq \frac{1}{2} \|d_t^{n,k}\|_n^2 + \frac{L^2}{2\varepsilon^2} \|d^{n,k-1}\|_n^2. \quad (62)$$

For term  $\frac{L^2}{2\varepsilon^2} \|d^{n,k-1}\|_n^2$ , by Lemma 1 and the fact  $d^{n,k-1}(t_{n-1}) = 0$ , we obtain

$$\frac{L^2}{2\varepsilon^2} \|d^{n,k-1}\|_n^2 \leq \frac{L^2 \tau^2}{2\varepsilon^2} \|d_t^{n,k-1}\|_n^2.$$

Combining the above two equations, we obtain

$$\|d_t^{n,k}\|_n^2 + \varepsilon \|\nabla d^{n,k}(t_n)\|^2 \leq \frac{L^2 \tau^2}{\varepsilon^2} \|d_t^{n,k-1}\|_n^2. \quad (63)$$

Thus, when  $\frac{L^2 \tau^2}{\varepsilon^2} < 1$ , the iteration leads to a contraction of  $\|d_t^{n,k}\|_n^2$  with rate  $\frac{L^2 \tau^2}{\varepsilon^2}$ . By the theorem on contracting maps, the iteration convergences.

**Remark 2.** *The above analysis shows the convergence of the iteration under the time step condition  $\tau \leq \varepsilon/L$ . Note that this is a sufficient condition, but may not be a necessary condition. One may develop adaptive time stepping method based on a posteriori error estimate of the numerical solution to use larger step sizes.*

#### 4.2. Uniqueness of solution to the implicit ESET scheme

The convergence of the iterative solver in last subsection ensures the existence of solutions to the implicit ESET scheme. Now we prove the uniqueness.

*Proof of the uniqueness part of Theorem 1.* Suppose equation (10) has two solutions  $h_1^n$  and  $h_2^n$ . Substituting the two solutions into the equation, then taking the difference, and denoting by  $w^n = h_1^n - h_2^n$ , we obtain

$$\int_{t_{n-1}}^{t_n} (w_t^n, v_t) + \varepsilon(\nabla w^n, \nabla v_t) + \frac{1}{\varepsilon}(f'(\zeta^n)(w^n), v_t) dt = 0, \quad \forall v \in V_{M,N}^{n,u^{n-1}}.$$

Then, by taking  $v = w^n$ , we get

$$\|w_t^n\|_n^2 + \frac{\varepsilon}{2}\|\nabla w^n(t_n)\| - \frac{\varepsilon}{2}\|\nabla w_t^n(t_{n-1})\| \leq \frac{L^2}{2\varepsilon^2}\|w^n\|_n^2 + \frac{1}{2}\|w_t^n\|_n^2. \quad (64)$$

Then, noticing that  $w^n(t_{n-1}) = 0$ , by using Lemma 1, one obtain

$$\frac{L^2}{2\varepsilon^2}\|w^n\|_n^2 \leq \frac{\tau^2 L^2}{2\varepsilon^2}\|w_t^n\|_n^2.$$

Combining the above results, we get

$$\left(1 - \frac{\tau^2 L^2}{\varepsilon^2}\right)\|w_t^n\|_n^2 + \varepsilon\|\nabla w^n(t_n)\| \leq 0. \quad (65)$$

So, when  $\tau < \varepsilon/L$ , we have  $\|w_t^n\|_n = 0$ . Then, the fact  $w^n(t_{n-1}) = 0$  leads to  $w^n \equiv 0$ .  $\square$

#### 4.3. Superconvergence of the implicit ESET scheme

The implicit ESET scheme indeed has a better convergence rate than the semi-implicit scheme due to superconvergence, which will be numerically demonstrated in next section. A lot of numerical schemes has been proved to have superconvergence for different applications [57, 58, 59, 60, 61, 62, 63, 64, 65]. Here we present a proof to the ESET scheme using a new boosting technique, which is helpful to better understand the superconvergence.

To analyze the superconvergence property, we first consider the spatial semi-discretization

$$(u_t^M, v) + \varepsilon(\nabla u^M, \nabla v) + (f(u^M), v) = 0, \quad \forall v \in V_M := P_M^0(\Omega). \quad (66)$$

A standard estimate will yields

$$\|u - u^M\| \leq C(t)\|u - \Pi_M^0 u\| \leq C(t)M^{-r}. \quad (67)$$

By assumption (34), we only need to consider temporal discretization error.

**Theorem 5.** *Let  $h^n$ ,  $u$  be the solution to (10) and (9), respectively. Denote by  $e^n(t) = h^n(t) - u(t)$ . Suppose  $f(u)$  satisfies*

$$\max_u |f'(u)| < L, \quad \max_u |f''(u)| < L_2. \quad (68)$$

*Then we have following superconvergence result*

$$\|e^n(t_n)\| \leq \mathcal{O}(\tau^{2N}), \quad n \geq 1, \quad \tau < \varepsilon/L. \quad (69)$$

*Proof.* 1) We consider the spatial-discretized Allen–Cahn equation, with  $u^M$  still denoted by  $u$ :

$$u_t - \varepsilon\Delta u + \frac{1}{\varepsilon}f(u) = \chi_M(t), \quad (70)$$

where  $\chi_M^n$  stands for residual of spatial Galerkin projection. Let  $u_r(t)$  be a smooth solution that is close to the exact solution  $u(t)$  with error bound  $\mathcal{O}(\tau^{N+1})$ , e.g.  $u_r|_{I_n} := \Pi_N^n \Pi_M^0 u$ . We consider the linear perturbation equation of (70) near  $u_r$  given below

$$v_t - \varepsilon \Delta v + \frac{1}{\varepsilon} f'(u_r) v = g(x, t). \quad (71)$$

We define operator  $A(t)$  as:  $A(t)v := -\varepsilon \Delta v + \frac{1}{\varepsilon} f'(u_r(t))v$ . Then the solution of (71) in  $I_n$  can be formulated as

$$v(t) = G(t_{n-1}, t)v(t_{n-1}) + \int_{t_{n-1}}^t G(s, t)g(x, s)ds, \quad (72)$$

where operator  $G(t_1, t_2) = e^{-\int_{t_1}^{t_2} A(s)ds}$ . We first prove the  $L^2$  stability of the operator  $G(s, t)$ . Consider (71) with  $g \equiv 0$ , pairing the equation with  $v$ , we obtain

$$\frac{1}{2} \frac{d}{dt} \|v\|^2 + \varepsilon \|\nabla v\|^2 \leq \frac{L}{\varepsilon} \|v\|^2, \quad t \in I_n.$$

Then application of Grönwall's inequality leads to

$$\|v(t)\|^2 \leq e^{2(t-t_{n-1})L/\varepsilon} \|v(t_{n-1})\|^2.$$

Then, by (72), the  $L^2$  operator norm of  $G$  is

$$\|G(s, t)\| \leq e^{(t-s)L/\varepsilon}. \quad (73)$$

2) Now suppose  $h^n$  is the ESET solution of (10), then

$$h_t^n - \varepsilon \Delta h^n + \frac{1}{\varepsilon} f(h^n) = \chi^n, \quad (74)$$

where  $\chi^n$  stands for space-time Galerkin projection residual, which means

$$(\chi^n, v)_n = 0, \quad \forall v \in V_{M, N-1}.$$

Taking the difference of (74) and (70), we have (we omit  $\chi_M(t)$  and a  $(u - u_r)^2$  term, since they are smaller than  $\mathcal{O}(\tau^{2N+1})$  by assumption and standard error estimate)

$$e_t^n - \varepsilon \Delta e^n + \frac{1}{\varepsilon} f'(u_r) e^n = \chi^n - \frac{1}{\varepsilon} f''(\zeta^n) (e^n)^2.$$

Then, by (72), we get

$$e^n(t) = G(t_{n-1}, t)e^n(t_{n-1}) + \int_{t_{n-1}}^t G(s, t) \left( \chi^n - \frac{1}{\varepsilon} f''(\zeta^n) (e^n(s))^2 \right) ds. \quad (75)$$

Taking the spatial norm on both sides, we get

$$\|e^n(t)\|^2 \leq 3 \|G(t_{n-1}, t)e^n(t_{n-1})\|^2 + 3 \left\| \int_{t_{n-1}}^t G(s, t) \chi^n ds \right\|^2 + \frac{3}{\varepsilon^2} \left\| \int_{t_{n-1}}^t G(s, t) f''(\zeta^n) (e^n(s))^2 ds \right\|^2. \quad (76)$$

For the first term on the right hand side of (76), we have

$$\|G(t_{n-1}, t)e^n(t_{n-1})\|^2 \leq e^{\frac{2(t-t_{n-1})L}{\varepsilon}} \|e^n(t_{n-1})\|^2. \quad (77)$$



For the last term on the right hand side of (76), we have

$$\begin{aligned} \left\| \int_{t_{n-1}}^t G(s, t) f''(\zeta^n) (e^n(s))^2 ds \right\|^2 &\leq \tau \int_{t_{n-1}}^t \|G(s, t) f''(\zeta^n) (e^n(s))^2\|^2 ds \\ &\leq \tau \int_{t_{n-1}}^t e^{\frac{2(t-s)L}{\varepsilon}} L_2^2 \|e^n(s)\|_{L^4}^4 ds \\ &\leq \tau e^{\frac{2\tau L}{\varepsilon}} L_2^2 \int_{t_{n-1}}^t K(\|\nabla e^n\| + \|e^n\|)^4 ds, \quad t \in I_n, \end{aligned}$$

where Sobolev embedding theorem is used in the last inequality. By Theorem 3,  $\|\nabla e^n\| + \|e^n\| \sim \mathcal{O}(\tau^{N+1})$ , thus

$$\left\| \int_{t_{n-1}}^t G(s, t) f''(\zeta^n) (e^n(s))^2 ds \right\|^2 \leq L_2^2 c_K e^{\frac{2\tau L}{\varepsilon}} \tau^{4N+6}, \quad t \in I_n, \quad (78)$$

where  $c_K$  is a constant independent of  $\tau$ .

For the second term on the right hand side of (76), we have (at  $t = t_n$ )

$$\int_{t_{n-1}}^{t_n} G(s, t_n) \chi^n(s) ds = \int_{t_{n-1}}^{t_n} (G(s, t_n) - v(s)) \chi^n(s) ds, \quad \forall v \in V_{M, N-1}^n. \quad (79)$$

Note that, since we are working in spatial-discretized equation,  $\chi^n$  can be regarded as a vector of time, both  $G$  and  $v$  can be regarded as matrices. We expand  $G(s, t_n)$  at  $s = t_n$ . Suppose

$$A(t) = \sum_{k=0}^{N-1} A^{(k)}(t_n) \frac{(t - t_n)^k}{k!} + \mathcal{O}(\tau^N).$$

Let  $Z = -\int_s^{t_n} A(t) dt$ , then

$$Z = -\sum_{k=0}^{N-1} \frac{A^{(k)}(t_n)}{k!} \int_s^{t_n} (t - t_n)^k dt + \mathcal{O}(\tau^{N+1}) = \sum_{k=0}^{N-1} \frac{A^{(k)}(t_n)}{(k+1)!} (s - t_n)^{k+1} + \mathcal{O}(\tau^{N+1}).$$

Then,  $Z = \mathcal{O}(\tau)$ , and

$$\begin{aligned} G(s, t_n) &= e^Z = \sum_{k=0}^{N-1} \frac{Z^k}{k!} + \mathcal{O}(\tau^N) \\ &= \sum_{k=0}^{N-1} \frac{1}{k!} \left( \sum_{j=0}^{N-1} \frac{A^{(j)}(t_n)}{(j+1)!} (s - t_n)^{j+1} \right)^k + \mathcal{O}(\tau^N) \\ &= \sum_{k=0}^{N-1} G^{(k)} (s - t_n)^k + \mathcal{O}(\tau^N). \end{aligned}$$

By symmetry,  $G^{(k)}$  is a symmetric diagonalizable matrix. We denote  $\{\lambda_i^{(k)}, \eta_i^{(k)}\}, i = 1, \dots, M$  as the eigen-pairs of  $G^{(k)}$ , i.e.

$$G^{(k)} = \sum_{i=1}^M \lambda_i^{(k)} \eta_i^{(k)} (\eta_i^{(k)})^T.$$

Suppose the Galerkin discretization using basis function  $\psi_j(x) \in V_M$ , then the eigen-functions are given by  $\varphi_i^{(k)}(x) = \sum_{j=1}^M \eta_{ij}^{(k)} \psi_j(x)$ . Let

$$v(t, x, y) = \sum_{k=0}^{N-1} \sum_{i=1}^M \lambda_i^{(k)} \varphi_i^{(k)}(y) \varphi_i^{(k)}(x) (s - t_n)^k \in V_{M, N-1}.$$

Then

$$G(s, t; x, y) - v(t, x, y) \sim \mathcal{O}(\tau^N).$$

And it is not hard to show that the residual error has a bound  $\|\chi^n\| \sim \mathcal{O}(\tau^N)$ . So we have

$$\left\| \int_{t_{n-1}}^t G(s, t) \chi^n ds \right\|^2 \leq \mathcal{O}(\tau^{4N+1}). \quad (80)$$

Combine (76), (77), (78) and (80), then use a discrete Grönwall's inequality, we obtain the superconvergence result.  $\square$

**Remark 3.** *As discussed in Remark 1, the standard double-well potential (4) doesn't satisfy condition (11). But the truncated quadratic growth potential (13) and (14) satisfies the Lipschitz condition (11) with  $L = 3M^2 - 1$  and  $L = 2$ , respectively. Actually, the second condition in (68) is satisfied almost everywhere with  $L_2 = 6M$  and  $L_2 = 6$ , respectively for potential (13) and (14). To have smaller  $L$  and  $L_2$ , we suggest to use (14) for the Allen-Cahn equation.*

## 5. Numerical results

In this section, we numerically verify the stability and accuracy of proposed schemes.

To test the numerical scheme, we first solve (1) in a one-dimensional domain  $\Omega = [-1, 1]$ . For the homogeneous Dirichlet boundary condition  $u|_{\partial\Omega} = 0$ , we take a reference solution

$$u_{\text{ref}} = \tanh\left(\frac{x-t}{\varepsilon}\right) - \frac{1}{2}[(x+1)\tanh\left(\frac{1-t}{\varepsilon}\right) + (1-x)\tanh\left(\frac{-1-t}{\varepsilon}\right)]. \quad (81)$$

Neumann boundary condition can be achieved similarly. Notice that the reference solution does not satisfy Allen-Cahn equation (1). We add an external force term into (1) to make (81) an exact solution.

First, we take  $T = 0.32, M = 255, \varepsilon = 0.05, S = 0, \tau = 0.01$  and use two different boundary conditions to test the stability and accuracy of the proposed schemes. The numerical results are given in Figure 1, from which we see the proposed scheme give good numerical solutions. Here ESET33 means using semi-implicit ESET scheme with  $N = 3$  (first 3 in ESET33) as an iterative solver for the implicit ESET scheme using 3 (second 3 in ESET33) iterations. From the analysis given in last section, we know that each iteration will increase the order of the numerical scheme by 1, until the maximum order (which is 6 for the implicit scheme with  $N = 3$ ) is achieved. Using more than 3 iterations can further increase the accuracy of numerical solutions a little bit, but the convergence order can't be improved.

We then test convergence rates and make comparison with well-known schemes. Several commonly used fourth order time marching schemes are investigated by Kassam and Trefethen [66], they found that the fourth order implicit-explicit backward differentiation formula (IMEX4), and the fourth order exponential time-differencing Runge-Kutta method (ETDRK4) give the best performance results. We compare our scheme with these two schemes. The convergence rates of the proposed implicit (ESET22, ESET33) and semi-implicit (ESET31) schemes together with IMEX4 and ETRK4 schemes are presented in the left plot of Figure 2. The results of numerical accuracy versus computer time for these schemes are given in the right plot of Figure 2. We find that ESET31, ESET22, IMEX4, ETDRK4 all have fourth order convergence, but ESET22 has the smallest error constant and is the most efficient one among these fourth order schemes in terms of computational cost, due to superconvergence. When high accuracy is needed, the 6th order ESET33 scheme out-perform all the fourth order schemes significantly.

Figure 3 presents the energy dissipation of ESET31 scheme (15) with different time step sizes and stabilization constants. We find that shortening the time step can stabilize the energy curve, and the stability constant is also helpful.

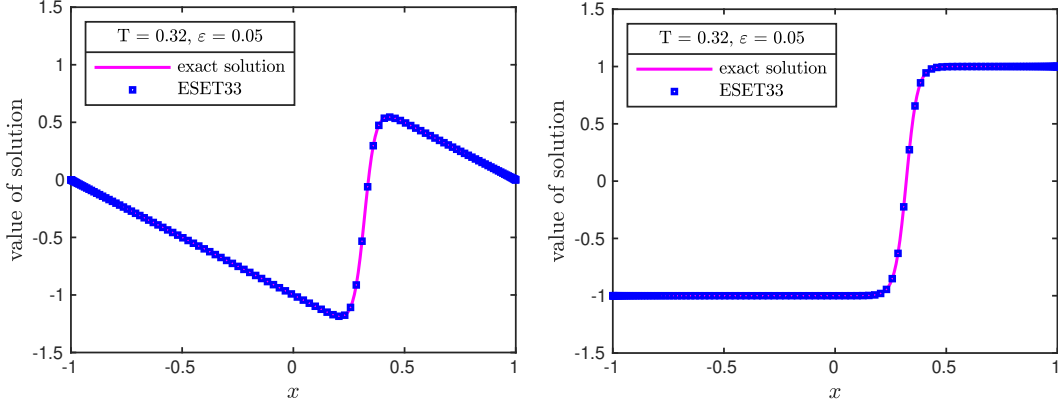


Figure 1: Testing ESET with Dirichlet(left) and Neumann(right) boundary condition, respectively. The scheme parameters used:  $M = 255$ ,  $N = 3$ ,  $\tau = 0.01$ ,  $S = 0$ .

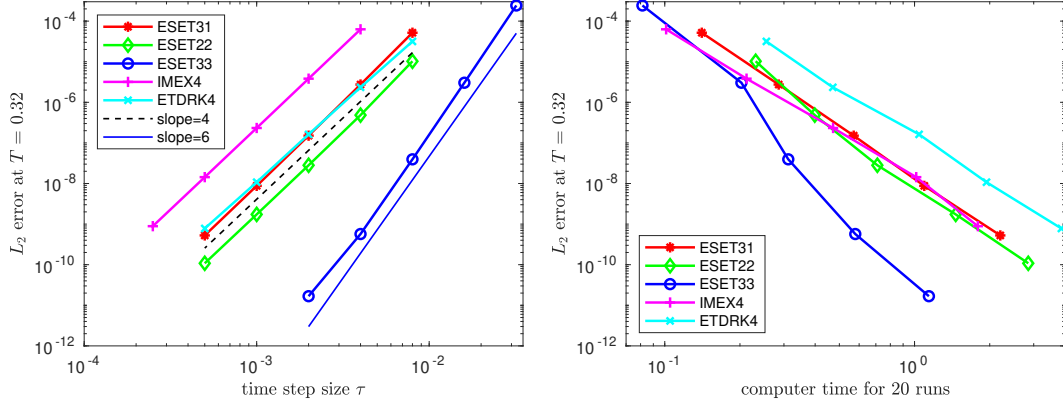


Figure 2: Accuracy and efficiency of ESET, IMEX4, and ETDK4 schemes. The common parameters used:  $\varepsilon = 0.05$ ,  $M = 350$ ,  $S = 0$ .

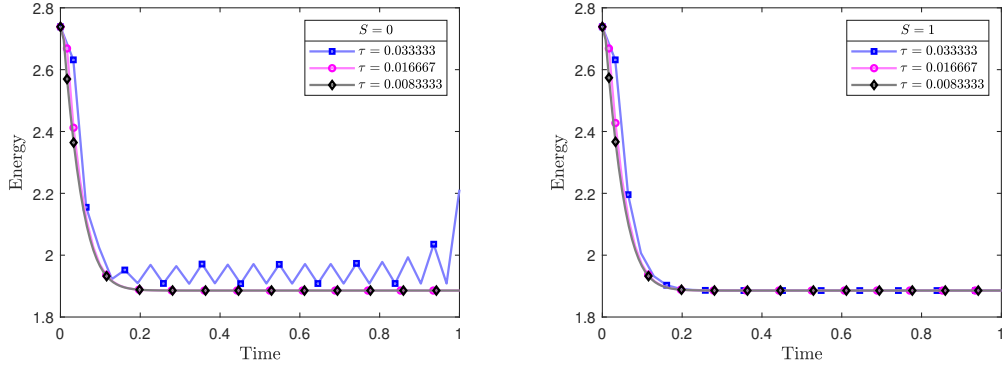


Figure 3: The energy dissipation of ESET31 scheme (15) with different stabilization constant  $S$  for  $\varepsilon = 0.08$  and  $M = 350$ .

In Figure 4, we investigate the effect on accuracy of stabilization and a simple cut-off operation to maintain maximum principle [67, 68]. From this figure, we see that the stabilization constant  $S$  can improve the stability when time step size is large, but will increase the numerical error a little bit when time step size is small and the stability is not an issue. This suggests that one should adjust the stability constant according to time step size [42]. On the other side, using cut-off increases both stability and accuracy, see the right plot of Figure 4.

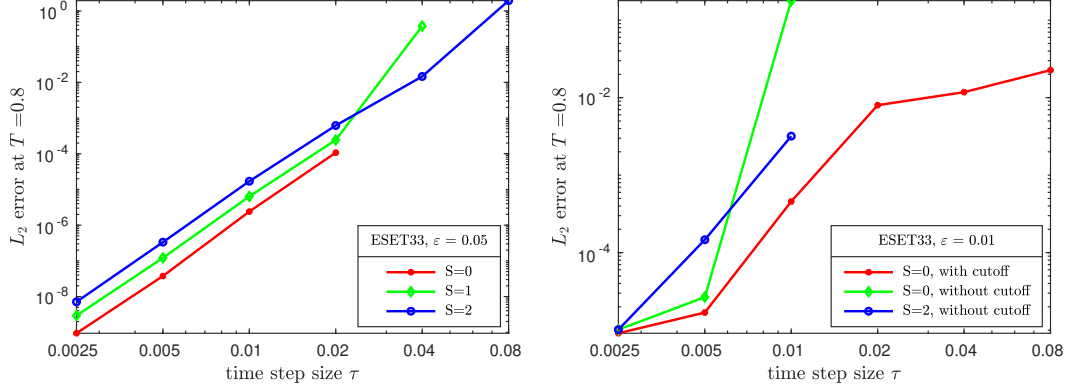


Figure 4: Effects on stability and accuracy of the stabilization constant and cut-off operation to maintain maximum principle.  $M = 350$ . In this figure, the lines break at a time step size when the corresponding numerical scheme encounters blow-ups.

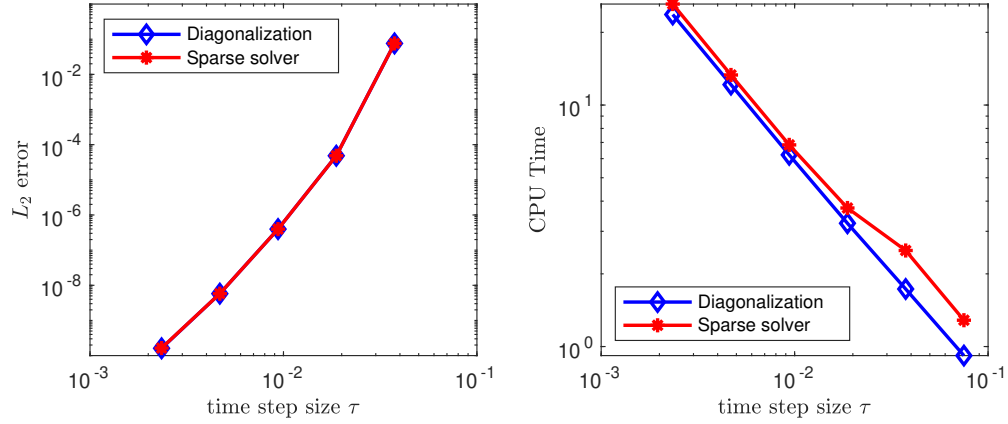


Figure 5: Comparison of accuracy and efficiency between the diagonalization method and direct sparse solver of the ESET42 scheme with  $M = 350$ ,  $\varepsilon = 0.08$ ,  $T = 1.2$ .

In Figure 5, we compare the performance of the direct sparse solver and the diagonalization approach in a ESET42 scheme. We see two solution methods give the same numerical solutions, and the diagonalization method use slightly less computer time.

Next we solve the conservative Allen–Cahn equation [69] in a two-dimensional domain  $\Omega = [-1, 1]^2$ :

$$\frac{\partial u}{\partial t}(x, t) - \varepsilon \Delta u(x, t) = -\frac{1}{\varepsilon} f(u(x, t)) + \alpha(t), \quad x \in \Omega, \quad (82)$$

where

$$\alpha(t) = \frac{1}{|\Omega|} \int_{\Omega} f(u(x, t)) dx, \quad (83)$$

is a non-local term to conserve total mass

$$\int_{\Omega} u(x, t) dx = \int_{\Omega} u(x, 0) dt.$$

The numerical scheme for (82) is almost the same as for the standard Allen–Cahn equation, since  $\alpha$  is a function depends only on  $f(u)$ .

More precisely, the semi-implicit ESET scheme for (82) reads: Find  $h^n \in V_{M,N}^{n, u^{n-1}}$ , s.t.

$$\int_{t_{n-1}}^{t_n} (h_t^n, v_t) + \varepsilon(\nabla h^n, \nabla v_t) + \left(\frac{1}{\varepsilon} f(\hat{h}^n) - \hat{\alpha}(t), v_t\right) dt = 0, \quad \forall v \in V_{M,N}^{n, u^{n-1}}, \quad (84)$$

where  $\hat{\alpha}(t) = \frac{1}{|\Omega|} \int_{\Omega} f(\hat{h}^n(x, t)) dx$ . By taking test function  $v_t \equiv 1$  in (84), we obtain the discrete mass conservation automatically.

We first use ESET22 to simulate a case with  $\varepsilon = 0.01$  and random initial value. The initial solution takes uniform random number  $U(0, 1)$  at each tensor product Legendre–Gauss quadrature point  $(x_i, y_j)$ :

$$h^0(x_i, y_j) \sim U(0, 1). \quad (85)$$

We use  $M = 280^2$  spatial bases, and set initial time step size to be  $\tau = 10^{-5}$ , then increase the time step to  $10^{-3}$  after calculating 99 steps. Figure 6 presents the snapshots of solutions of conservative Allen–Cahn equation together with standard Allen–Cahn equation with the same initial condition for comparison. We observe that for conserved case, phase separation happened in a very short time, while one phase gets dominant in the non-conserved case. The corresponding mass conservation and energy dissipation are presented in Figure 7, from which we observe that the total mass is kept up to machine accuracy for the conservative Allen–Cahn equation, but no mass conservation for the standard Allen–Cahn equation, which are consistent with the results shown in Figure 6. We observe that both cases dissipate energy.

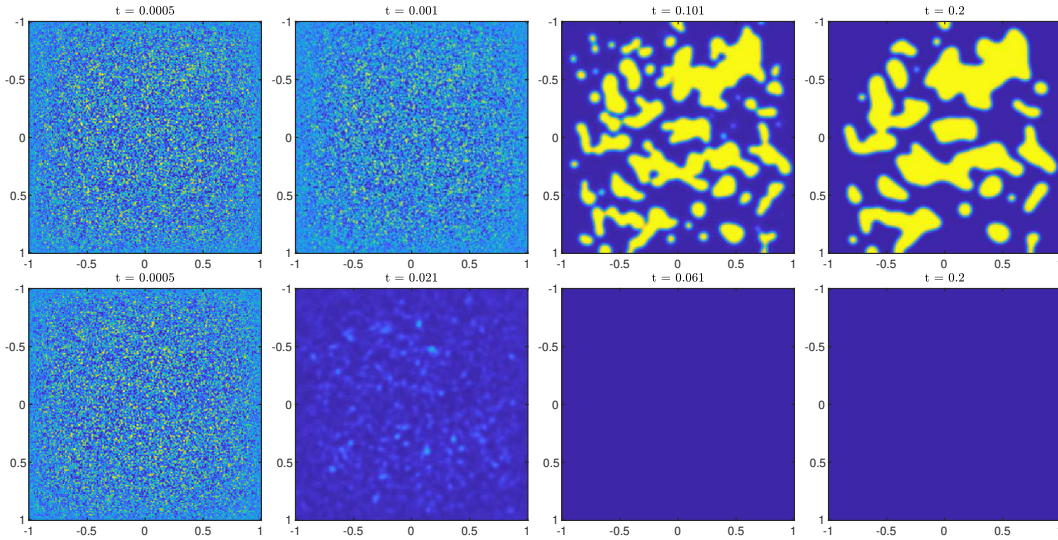


Figure 6: Solution snapshots of conservative Allen–Cahn equation (*top*) and standard Allen–Cahn equation (*bottom*) for random initial condition (85) by the ESET22 scheme.  $\varepsilon = 0.01$ ,  $M = 280^2$ ,  $T = 0.2$ ,  $S = 0$ .

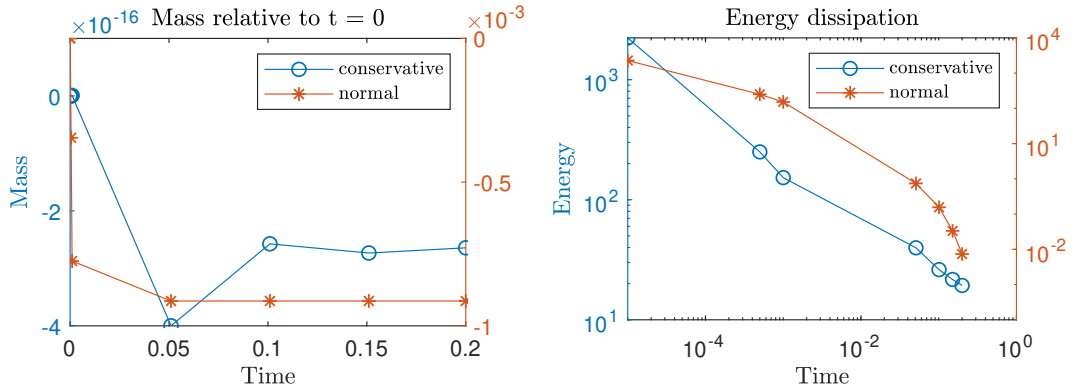


Figure 7: Mass changes (left) and energy dissipation (right) of the conservative Allen–Cahn equation and standard (normal) Allen–Cahn equation for random initial condition (85) by the ESET22 scheme.  $\varepsilon = 0.01$ ,  $M = 280^2$ ,  $T = 0.2$ ,  $S = 0$ .

Next, we simulate drop coalescence with initial state contains two balls centered at  $(0.4, 0)$  and  $(-0.4, 0)$  with radius 0.38. We use same solver ESET22 to solve the standard and conservative Allen–Cahn equations. The results are presented in Figure 8, 9 and 10. We observe that in the conserved case, two balls merge into one larger ball, the total mass is kept; but in standard case, the two balls first merge then disappear at an almost constant rate of total mass diminishing. Both cases dissipate energy.

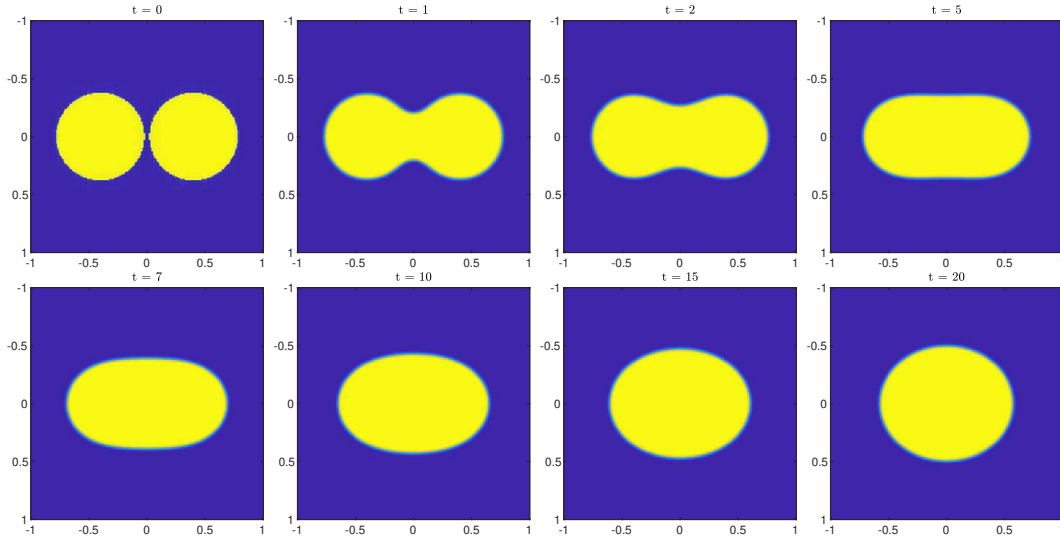


Figure 8: Snapshots of conservative Allen–Cahn equation for the drop coalescence test using ESET22 scheme with  $\tau = 5 \times 10^{-3}$ ,  $M = 280^2$ ,  $\varepsilon = 0.01$ ,  $T = 20$ .

## 6. Concluding remarks

Based on an energetic variational formulation, we proposed two efficient spectral-element time marching methods for nonlinear gradient systems: one implicit ESET scheme and one semi-implicit ESET scheme. The semi-implicit ESET scheme leads to linear systems with constant coefficients, thus can be efficiently solved. The implicit ESET scheme has superconvergence property, it can be efficiently solved by using the semi-implicit scheme as an iterative solver. There are several advantages of the

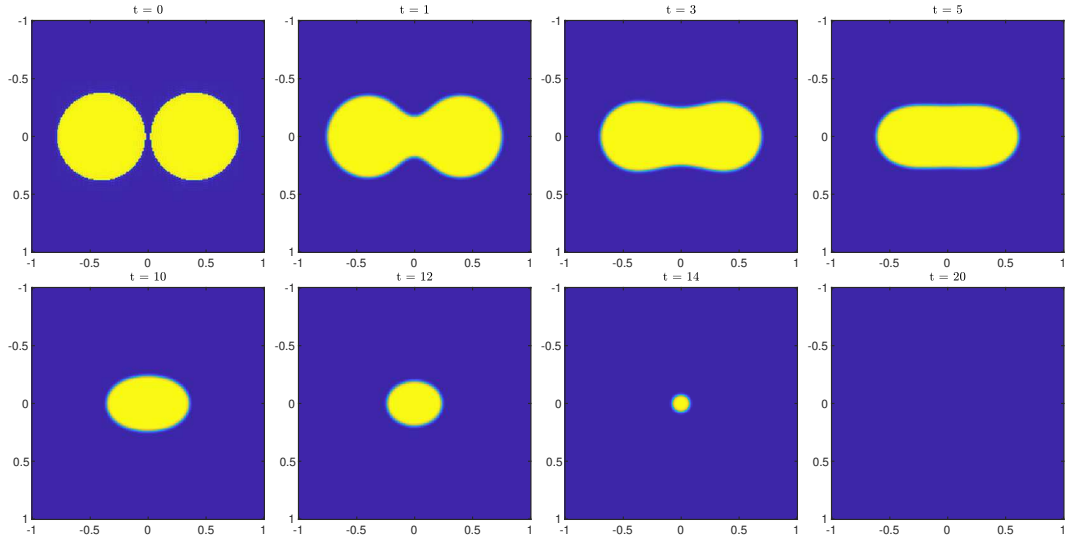


Figure 9: Snapshots of standard Allen–Cahn equation for the drop coalescence test using ESET22 scheme with  $\tau = 5 \times 10^{-3}$ ,  $M = 280^2$ ,  $\varepsilon = 0.01$ ,  $T = 20$ .

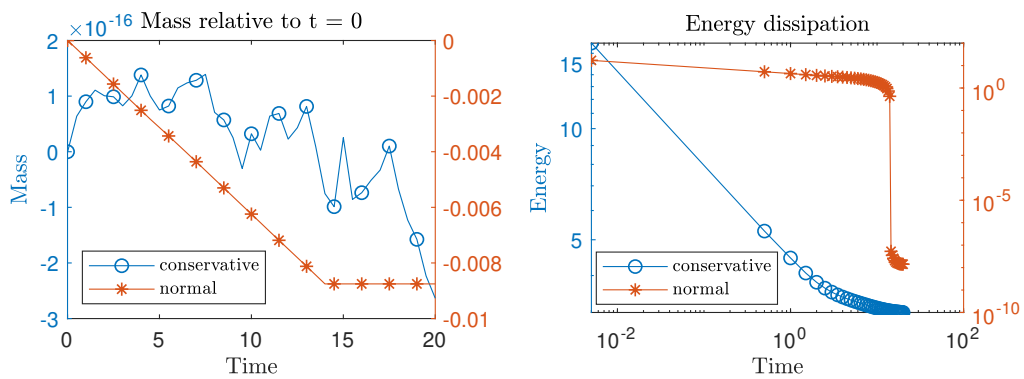


Figure 10: Mass changes (left) and energy dissipation (right) of conservative and standard (normal) Allen–Cahn equations for the drop coalescence test obtained by ESET22 scheme with  $\tau = 5 \times 10^{-3}$ ,  $M = 280^2$ ,  $\varepsilon = 0.01$ ,  $T = 20$ .

proposed schemes: 1) They keep mass conservation accurately if the continuous equation conserves mass. 2) They keep the energy dissipation with a time step size related to physical time scale. 3) They are high order accurate and efficient. In particular, when using the semi-implicit scheme as an iterative solver for the fully implicit scheme, superconvergence can be achieved, resulting a more efficient method than existing ones. 4) The diagonalization solution procedure allows the method to be used for large scale problems with parallel computing in time.

In this paper, we only considered the Allen–Cahn equations. But the proposed methods can be used for other parabolic type nonlinear systems. However, application to  $H^{-1}$  gradient systems, e.g. the Cahn–Hilliard equation is not trivial, direct extension without a good stabilization leads to a scheme with time step size restriction of order  $\mathcal{O}(\varepsilon^3)$ . How to design unconditionally stable linear ESET schemes for Allen–Cahn type and Cahn–Hilliard type equations deserves a further study.

### CRediT authorship contribution statement

Shiqin Liu: Conceptualization, Formal analysis, Investigation, Methodology, Writing. Haijun Yu: Conceptualization, Formal analysis, Investigation, Methodology, Writing, Funding acquisition.

### Declaration of competing interest

We declare that we have no financial and personal relationships with other people or organizations that can inappropriately influence our work. There is no professional or other personal interest of any nature or kind in any product, service and/or company that could be construed as influencing the position presented in, or the review of, the manuscript entitled.

### Acknowledgments

This work was partially supported by the National Natural Science Foundation of China (grant number 12171467, 12161141017). The computations were partially done on the high-performance computers of the State Key Laboratory of Scientific and Engineering Computing, Chinese Academy of Sciences.

### References

- [1] J. W. Cahn, J. E. Hilliard, Free energy of a nonuniform system. I. Interfacial free energy, *J. Chem. Phys.* 28 (2) (1958) 258–267. [doi:10.1063/1.1744102](https://doi.org/10.1063/1.1744102).
- [2] S. M. Allen, J. W. Cahn, A microscopic theory for antiphase boundary motion and its application to antiphase domain coarsening, *Acta Met. Mater* 27 (1979) 1085–1095. [doi:10.1016/0001-6160\(79\)90196-2](https://doi.org/10.1016/0001-6160(79)90196-2).
- [3] L.-Q. Chen, Phase-field models for microstructure evolution, *Annu. Rev. Mater. Res.* 32 (1) (2002) 113–140. [doi:10.1146/annurev.matsci.32.112001.132041](https://doi.org/10.1146/annurev.matsci.32.112001.132041).
- [4] M. Greenwood, N. Provatas, J. Rottler, Free energy functionals for efficient phase field crystal modeling of structural phase transformations, *Phys. Rev. Lett.* 105 (4) (2010). [doi:10.1103/PhysRevLett.105.045702](https://doi.org/10.1103/PhysRevLett.105.045702).
- [5] D. M. Anderson, G. B. McFadden, A. A. Wheeler, Diffuse-interface methods in fluid mechanics, *Annu. Rev. Fluid Mech.* 30 (1) (1998) 139–165. [doi:10.1146/annurev.fluid.30.1.139](https://doi.org/10.1146/annurev.fluid.30.1.139).
- [6] J. Lowengrub, L. Truskinovsky, Quasi-incompressible Cahn–Hilliard fluids and topological transitions, *Proceedings: Mathematical, Physical and Engineering Sciences* 454 (1978) (1998) 2617–2654. [arXiv:53238](https://arxiv.org/abs/53238), [doi:10.1098/rspa.1998.0273](https://doi.org/10.1098/rspa.1998.0273).



- [7] P. Yue, J. J. Feng, C. Liu, J. Shen, A diffuse-interface method for simulating two-phase flows of complex fluids, *J. Fluid Mech.* 515 (2004) 293–317. doi:[10.1017/S0022112004000370](https://doi.org/10.1017/S0022112004000370).
- [8] T. Qian, X.-P. Wang, P. Sheng, A variational approach to moving contact line hydrodynamics, *J. Fluid Mech.* 564 (2006) 333–360. doi:[10.1017/S0022112006001935](https://doi.org/10.1017/S0022112006001935).
- [9] Q. Du, C. Liu, X. Wang, A phase field approach in the numerical study of the elastic bending energy for vesicle membranes, *J. Comput. Phys.* 198 (2) (2004) 450–468. doi:[10.1016/j.jcp.2004.01.029](https://doi.org/10.1016/j.jcp.2004.01.029).
- [10] J. T. Oden, A. Hawkins, S. Prudhomme, General diffuse-interface theories and an approach to predictive tumor growth modeling, *Math. Models Methods Appl. Sci.* 20 (03) (2010) 477–517. doi:[10.1142/S0218202510004313](https://doi.org/10.1142/S0218202510004313).
- [11] S. M. Wise, J. S. Lowengrub, H. B. Frieboes, V. Cristini, Three-dimensional multispecies nonlinear tumor growth I: Model and numerical method, *J. Theor. Biol.* 253 (3) (2008) 524–543. doi:[10.1016/j.jtbi.2008.03.027](https://doi.org/10.1016/j.jtbi.2008.03.027).
- [12] A. Miranville, E. Rocca, G. Schimperna, On the long time behavior of a tumor growth model, *J. Differ. Equations* 267 (4) (2019) 2616–2642. doi:[10.1016/j.jde.2019.03.028](https://doi.org/10.1016/j.jde.2019.03.028).
- [13] C. Liu, J. Shen, A phase field model for the mixture of two incompressible fluids and its approximation by a Fourier-spectral method, *Physica D* 179 (3-4) (2003) 211–228. doi:[10.1016/S0167-2789\(03\)00030-7](https://doi.org/10.1016/S0167-2789(03)00030-7).
- [14] Q. Du, R. A. Nicolaides, Numerical analysis of a continuum model of phase transition, *SIAM J. Numer. Anal.* 28 (5) (1991) 1310–1322. doi:[10.1137/0728069](https://doi.org/10.1137/0728069).
- [15] C. M. Elliott, A. M. Stuart, The global dynamics of discrete semilinear parabolic equations, *SIAM J. Numer. Anal.* 30 (6) (1993) 1622–1663. doi:[10.1137/0730084](https://doi.org/10.1137/0730084).
- [16] D. J. Eyre, Unconditionally gradient stable time marching the Cahn–Hilliard equation, *MRS Proc.* 529 (1998) 39. doi:[10.1557/PROC-529-39](https://doi.org/10.1557/PROC-529-39).
- [17] C. Wang, S. M. Wise, An energy stable and convergent finite-difference scheme for the modified phase field crystal equation, *SIAM J. Numer. Anal.* 49 (3) (2011) 945–969. doi:[10.1137/090752675](https://doi.org/10.1137/090752675).
- [18] J. Shen, C. Wang, X. Wang, S. M. Wise, Second-order convex splitting schemes for gradient flows with Ehrlich–Schwoebel type energy: Application to thin film epitaxy, *SIAM J. Numer. Anal.* 50 (1) (2012) 105–125. doi:[10.1137/110822839](https://doi.org/10.1137/110822839).
- [19] L. Chen, J. Shen, Applications of semi-implicit Fourier-spectral method to phase field equations, *Comput. Phys. Commun.* 108 (2-3) (1998) 147–158. doi:[10.1016/S0010-4655\(97\)00115-X](https://doi.org/10.1016/S0010-4655(97)00115-X).
- [20] J. Zhu, L.-Q. Chen, J. Shen, V. Tikare, Coarsening kinetics from a variable-mobility Cahn–Hilliard equation: Application of a semi-implicit Fourier spectral method, *Phys. Rev. E* 60 (4) (1999) 3564–3572. doi:[10.1103/PhysRevE.60.3564](https://doi.org/10.1103/PhysRevE.60.3564).
- [21] C. Xu, T. Tang, Stability analysis of large time-stepping methods for epitaxial growth models, *SIAM J. Numer. Anal.* 44 (4) (2006) 1759–1779. doi:[10.1137/050628143](https://doi.org/10.1137/050628143).
- [22] J. Shen, X. Yang, Numerical approximations of Allen–Cahn and Cahn–Hilliard equations, *Discrete Cont. Dyn. A* 28 (4) (2010) 1669–1691. doi:[10.3934/dcds.2010.28.1669](https://doi.org/10.3934/dcds.2010.28.1669).
- [23] L. Wang, H. Yu, On efficient second order stabilized semi-implicit schemes for the Cahn–Hilliard phase-field equation, *J. Sci. Comput.* 77 (2) (2018) 1185–1209. doi:[10.1007/s10915-018-0746-2](https://doi.org/10.1007/s10915-018-0746-2).

- [24] L. Wang, H. Yu, An energy stable linear diffusive Crank–Nicolson scheme for the Cahn–Hilliard gradient flow, *J. Comput. Appl. Math.* 377 (2020) 112880. doi:[10.1016/j.cam.2020.112880](https://doi.org/10.1016/j.cam.2020.112880).
- [25] X. Li, Z. Qiao, C. Wang, Double stabilizations and convergence analysis of a second-order linear numerical scheme for the nonlocal Cahn–Hilliard equation, *Sci. China Math.* (2023). doi:[10.1007/s11425-022-2036-8](https://doi.org/10.1007/s11425-022-2036-8).
- [26] R. Guo, F. Filbet, Y. Xu, Efficient high order semi-implicit time discretization and local discontinuous Galerkin methods for highly nonlinear PDEs, *J. Sci. Comput.* 68 (3) (2016) 1029–1054. doi:[10.1007/s10915-016-0170-4](https://doi.org/10.1007/s10915-016-0170-4).
- [27] X. Wang, L. Ju, Q. Du, Efficient and stable exponential time differencing Runge–Kutta methods for phase field elastic bending energy models, *J. Comput. Phys.* 316 (2016) 21–38. doi:[10.1016/j.jcp.2016.04.004](https://doi.org/10.1016/j.jcp.2016.04.004).
- [28] L. Zhu, L. Ju, W. Zhao, Fast high-order compact exponential time differencing Runge–Kutta methods for second-order semilinear parabolic equations, *J. Sci. Comput.* 67 (3) (2016) 1043–1065. doi:[10.1007/s10915-015-0117-1](https://doi.org/10.1007/s10915-015-0117-1).
- [29] J. Shin, H. G. Lee, J.-Y. Lee, Unconditionally stable methods for gradient flow using convex splitting Runge–Kutta scheme, *J. Comput. Phys.* 347 (2017) 367–381. doi:[10.1016/j.jcp.2017.07.006](https://doi.org/10.1016/j.jcp.2017.07.006).
- [30] H. Zhang, J. Yan, X. Qian, X. Chen, S. Song, Explicit third-order unconditionally structure-preserving schemes for conservative Allen–Cahn equations, *J. Sci. Comput.* 90 (1) (2021) 8. doi:[10.1007/s10915-021-01691-w](https://doi.org/10.1007/s10915-021-01691-w).
- [31] L. Ju, X. Li, Z. Qiao, J. Yang, Maximum bound principle preserving integrating factor Runge–Kutta methods for semilinear parabolic equations, *J. Comput. Phys.* 439 (2021) 110405. arXiv:[2010.12165](https://arxiv.org/abs/2010.12165), doi:[10.1016/j.jcp.2021.110405](https://doi.org/10.1016/j.jcp.2021.110405).
- [32] Z. Fu, T. Tang, J. Yang, Energy plus maximum bound preserving Runge–Kutta methods for the Allen–Cahn equation, *J. Sci. Comput.* 92 (3) (2022) 97. arXiv:[2203.04784](https://arxiv.org/abs/2203.04784), doi:[10.1007/s10915-022-01940-6](https://doi.org/10.1007/s10915-022-01940-6).
- [33] X. Yang, J. Zhao, X. He, Linear, second order and unconditionally energy stable schemes for the viscous Cahn–Hilliard equation with hyperbolic relaxation using the invariant energy quadratization method, *J. Comput. Appl. Math.* 343 (2018) 80–97. doi:[10.1016/j.cam.2018.04.027](https://doi.org/10.1016/j.cam.2018.04.027).
- [34] X. Yang, H. Yu, Efficient second order unconditionally stable schemes for a phase field moving contact line model using an invariant energy quadratization approach, *SIAM J. Sci. Comput.* 40 (3) (2018) B889–B914. doi:[10.1137/17M1125005](https://doi.org/10.1137/17M1125005).
- [35] X. Yang, G.-D. Zhang, Convergence analysis for the invariant energy quadratization (IEQ) schemes for solving the Cahn–Hilliard and Allen–Cahn equations with general nonlinear potential, *J. Sci. Comput.* 82 (3) (2020) 55. doi:[10.1007/s10915-020-01151-x](https://doi.org/10.1007/s10915-020-01151-x).
- [36] F. Guillén-González, G. Tierra, On linear schemes for a Cahn–Hilliard diffuse interface model, *J. Comput. Phys.* 234 (2013) 140–171. doi:[10.1016/j.jcp.2012.09.020](https://doi.org/10.1016/j.jcp.2012.09.020).
- [37] F. Guillén-González, G. Tierra, Second order schemes and time-step adaptivity for Allen–Cahn and Cahn–Hilliard models, *Comput. Math. Appl.* 68 (8) (2014) 821–846. doi:[10.1016/j.camwa.2014.07.014](https://doi.org/10.1016/j.camwa.2014.07.014).
- [38] J. Shen, J. Xu, J. Yang, A new class of efficient and robust energy stable schemes for gradient flows, *SIAM Rev.* 61 (3) (2019) 474–506. doi:[10.1137/17M1150153](https://doi.org/10.1137/17M1150153).

- [39] J. Shen, J. Xu, J. Yang, The scalar auxiliary variable (SAV) approach for gradient flows, *J. Comput. Phys.* 353 (2018) 407–416. doi:10.1016/j.jcp.2017.10.021.
- [40] J. Shen, J. Xu, Convergence and error analysis for the scalar auxiliary variable (SAV) schemes to gradient flows, *SIAM J. Numer. Anal.* 56 (5) (2018) 2895–2912. doi:10.1137/17M1159968.
- [41] X. Feng, A. Prohl, Numerical analysis of the Allen–Cahn equation and approximation for mean curvature flows, *Numer. Math.* 94 (1) (2003) 33–65. doi:10.1007/s00211-002-0413-1.
- [42] L. Wang, H. Yu, Energy-stable second-order linear schemes for the Allen–Cahn phase-field equation, *Commun. Math. Sci.* 17 (3) (2019) 609–635. doi:20190830152653.
- [43] J.-g. Tang, H.-p. Ma, Single and multi-interval Legendre spectral methods in time for parabolic equations, *Numer. Meth. Part. D. E.* 22 (5) (2006) 1007–1034. doi:10.1002/num.20135.
- [44] J. Shen, L.-L. Wang, Fourierization of the Legendre–Galerkin method and a new space-time spectral method, *Appl. Numer. Math.* 57 (5) (2007) 710–720. doi:10.1016/j.apnum.2006.07.012.
- [45] D. Kessler, R. H. Nochetto, A. Schmidt, A posteriori error control for the Allen–Cahn problem: Circumventing Gronwall’s inequality, *ESAIM Math. Model. Numer. Anal.* 38 (01) (2004) 129–142. doi:10.1051/m2an:2004006.
- [46] N. Condatte, C. Melcher, E. Süli, Spectral approximation of pattern-forming nonlinear evolution equations with double-well potentials of quadratic growth, *Math. Comp.* 80 (273) (2011) 205–223. doi:10.1090/S0025-5718-10-02365-3.
- [47] J. Shen, C.-T. Sheng, An efficient space-time method for time fractional diffusion equation, *J. Sci. Comput.* 81 (2) (2019) 1088–1110. doi:10.1007/s10915-019-01052-8.
- [48] J. Shen, Efficient spectral-Galerkin method I. Direct solvers of second- and fourth-order equations using Legendre polynomials, *SIAM J. Sci. Comput.* 15 (6) (1994) 1489. doi:10.1137/0915089.
- [49] H. Yu, X. Yang, Numerical approximations for a phase-field moving contact line model with variable densities and viscosities, *J. Comput. Phys.* 334 (2017) 665–686. doi:10.1016/j.jcp.2017.01.026.
- [50] L. Wang, H. Yu, Convergence analysis of an unconditionally energy stable linear Crank–Nicolson scheme for the Cahn–Hilliard equation, *J. Math. Study* 51 (1) (2018) 89–114. doi:10.4208/jms.v51n1.18.06.
- [51] J.-g. Tang, H.-p. Ma, Single and multi-interval legendre  $\tau$ -methods in time for parabolic equations, *Adv. Comput. Math.* 17 (4) (2002) 349–367. doi:10.1023/A:1016273820035.
- [52] R. E. Lynch, J. R. Rice, D. H. Thomas, Direct solution of partial difference equations by tensor product methods, *Numer. Math.* 6 (1) (1964) 185–199. doi:10.1007/BF01386067.
- [53] D. Kong, J. Shen, L.-L. Wang, S. Xiang, Eigenvalue analysis and applications of the Legendre dual-Petrov–Galerkin methods for initial value problems, arXiv:2211.10599 (2022).
- [54] Z. Chen, Y. Liu, Efficient and parallel solution of high-order continuous time Galerkin for dissipative and wave propagation problems, arXiv:2303.05008 (2023). doi:10.48550/arXiv.2303.05008.
- [55] J. Shen, T. Tang, L.-L. Wang, Spectral Methods: Algorithms, Analysis and Applications, no. 41 in Springer Series in Computational Mathematics, Springer, Heidelberg ; New York, 2011.

- [56] C. Canuto, M. Y. Hussaini, A. Quarteroni, T. A. Zang, Spectral Methods: Fundamentals in Single Domains, Springer Science & Business Media, 2007.
- [57] T. Dupont, A unified theory of superconvergence for Galerkin methods for two-point boundary problems, *SIAM J. Numer. Anal.* 13 (3) (1976) 362–368. doi:[10.1137/0713032](https://doi.org/10.1137/0713032).
- [58] D. N. Arnold, J. Douglas, Superconvergence of the Galerkin approximation of a quasilinear parabolic equation in a single space variable, *Calcolo* 16 (4) (1979) 345–369. doi:[10.1007/BF02576636](https://doi.org/10.1007/BF02576636).
- [59] T. Tang, Superconvergence of numerical solutions to weakly singular Volterra integro-differential equations, *Numer. Math.* 61 (1) (1992) 373–382. doi:[10.1007/BF01385515](https://doi.org/10.1007/BF01385515).
- [60] A. Zhou, Q. Lin, Optimal and superconvergence estimates of the finite element method for a scalar hyperbolic equation, *Acta Math. Sci.* 14 (1) (1994) 90–94. doi:[10.1016/S0252-9602\(18\)30094-8](https://doi.org/10.1016/S0252-9602(18)30094-8).
- [61] O. Karakashian, C. Makridakis, A space-time finite element method for the nonlinear Schrödinger equation: The continuous Galerkin method, *SIAM J. Numer. Anal.* 36 (6) (1999) 1779–1807. doi:[10.1137/S0036142997330111](https://doi.org/10.1137/S0036142997330111).
- [62] Z. Zhang, Superconvergence of spectral collocation and  $p$ -version methods in one dimensional problems, *Math. Comp.* 74 (252) (2005) 1621–1636. doi:[10.1090/S0025-5718-05-01756-4](https://doi.org/10.1090/S0025-5718-05-01756-4).
- [63] Q. Huang, H. Xie, H. Brunner, Superconvergence of discontinuous Galerkin solutions for delay differential equations of pantograph type, *SIAM J. Sci. Comput.* 33 (5) (2011) 2664–2684. doi:[10.1137/110824632](https://doi.org/10.1137/110824632).
- [64] Q. Gu, Y. Chen, Y. Huang, Superconvergence analysis of a two-grid finite element method for nonlinear time-fractional diffusion equations, *Comp. Appl. Math.* 41 (8) (2022) 361. doi:[10.1007/s40314-022-02070-3](https://doi.org/10.1007/s40314-022-02070-3).
- [65] M. Zhang, L. Yi, Superconvergent postprocessing of the continuous Galerkin time stepping method for nonlinear initial value problems with application to parabolic problems, *J. Sci. Comput.* 94 (2) (2023) 31. doi:[10.1007/s10915-022-02086-1](https://doi.org/10.1007/s10915-022-02086-1).
- [66] Kassam, Trefethen, Fourth-order time-stepping for stiff PDEs, *SIAM J. Sci. Comput.* 26 (4) (2005) 1214–1233. doi:[10.1137/s1064827502410633](https://doi.org/10.1137/s1064827502410633).
- [67] B. Li, J. Yang, Z. Zhou, Arbitrarily high-order exponential cut-off methods for preserving maximum principle of parabolic equations, *SIAM J. Sci. Comput.* 42 (6) (2020) A3957–A3978. doi:[10.1137/20M1333456](https://doi.org/10.1137/20M1333456).
- [68] J. Yang, Z. Yuan, Z. Zhou, Arbitrarily high-order maximum bound preserving schemes with cut-off postprocessing for Allen–Cahn equations, *J. Sci. Comput.* 90 (2) (2022) 76. doi:[10.1007/s10915-021-01746-y](https://doi.org/10.1007/s10915-021-01746-y).
- [69] J. Rubinstein, P. Sternberg, Nonlocal reaction-diffusion equations and nucleation, *IMA J. Appl. Math.* 48 (3) (1992) 249–264. doi:[10.1093/imamat/48.3.249](https://doi.org/10.1093/imamat/48.3.249).